inhibitory effect of pemetrexed on cell growth (Figure 2B). These data thus indicated that high TS expression levels reduce the sensitivity of NSCLC cells to pemetrexed.

Effects of chemotherapeutic agents on DNA synthesis and apoptosis in TS-overexpressing NSCLC cell lines

We next investigated the effects of TS overexpression on DNA synthesis and apoptosis in NSCLC cells exposed to pemetrexed, given that the cytotoxic activity of pemetrexed is due to inhibition of DNA synthesis and subsequent induction of apoptosis. Assay of BrdU incorporation revealed that pemetrexed inhibited DNA synthesis in Mock cell lines in a concentration-dependent manner, whereas this effect was much less pronounced in the TS-overexpressing lines (Figure 3A). In contrast, the concentration-dependent inhibition of DNA synthesis by cisplatin was largely unaffected by forced expression of TS (Figure 3B). An annexin V binding assay also revealed that the frequency of apoptosis was markedly increased by pemetrexed in a concentration-dependent manner in Mock cells, whereas pemetrexed had little effect on apoptosis in cells overexpressing TS (Figure 4A). To confirm that this attenuation of pemetrexed-induced apoptosis in TS-overexpressing cells was due to the forced expression of TS, we depleted the TS-overexpressing cells of TS by transfection with the TS siRNA and then examined the effect of pemetrexed on apoptosis. Downregulation of TS expression restored the sensitivity of these cells to the proapoptotic effect of pemetrexed. In contrast to pemetrexed, cisplatin increased the proportion of apoptotic cells among Mock and TS-overexpressing cells to similar extents (Figure 4C). These data thus suggested that the effects of pemetrexed on DNA synthesis and apoptosis are inversely related to the level of TS expression.

Effects of pemetrexed on the growth of TS-overexpressing NSCLC cells *in vivo*

We next investigated whether TS-overexpressing NSCLC cell lines might exhibit resistance to pemetrexed treatment in xenograft models. When their tumours became palpable, athymic nude mice were divided into two groups and treated with vehicle or pemetrexed for 3–4 weeks. Although pemetrexed significantly inhibited the growth of tumours formed by Mock cells of the A549, H1299, or PC9 lines, it did not exhibit such an effect with tumours formed by the corresponding TS-overexpressing cells (Figure 5). These data thus suggested that the antitumour effect of pemetrexed is suppressed by TS overexpression in NSCLC cells, consistent with our results obtained *in vitro*.

TS expression in tumours of NSCLC patients treated with pemetrexed

To evaluate the relation between the level of TS expression in NSCLC tumours and the clinical response to pemetrexed, we performed semiquantitative immunohistochemical analysis on tumour biopsy specimens from 24 patients with advanced NSCLC treated with pemetrexed combined with platinum agents

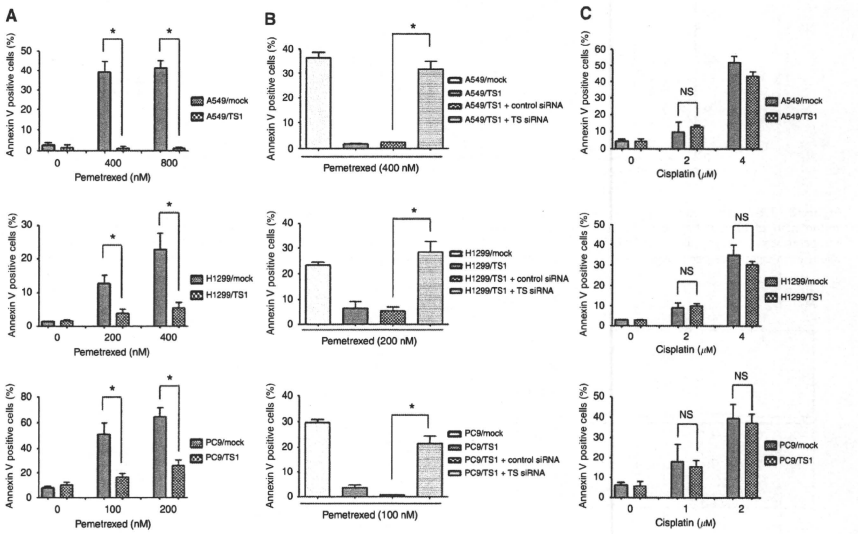

Figure 4 Effects of pemetrexed and cisplatin on apoptosis in NSCLC cells overexpressing TS. (**A** and **C**) The indicated NSCLC cell lines were cultured for 72 h in complete medium containing various concentrations of pemetrexed (**A**) or cisplatin (**C**), after which the proportion of apoptotic cells was assessed by staining with fluorescein isothiocyanate-conjugated annexin V and propidium iodide followed by flow cytometry. (**B**) The indicated NSCLC cell lines were cultured for 72 h in complete medium containing the indicated concentrations of pemetrexed with or without nonspecific (control) or TS siRNAs, after which the proportion of apoptotic cells was assessed as in **A** and **C**. All data are means ± s.d. of triplicates from experiments that were repeated a total of three times with similar results. *$P<0.05$ (Student's two-tailed *t*-test). NS, not significant.

(Figure 6A). The characteristics of the patients are shown in Table 2. Tumours were categorised as either responding (CR or PR) or non-responding (SD or PD). The level of TS expression for non-responding groups was significantly ($P = 0.038$) higher than that for responding groups (Figure 6B). We next carried out ROC curve analysis to establish the optimal cutoff value for the HSCORE of TS expression level, yielding a value of 257.5. Patients with a low level of TS expression (HSCORE$<$257.5) had a significantly longer progression-free survival ($P = 0.014$) than did those with a high level (HSCORE$\geqslant$257.5) (Figure 6C). These data thus suggested that TS expression level in advanced NSCLC tumours is inversely correlated with the response to pemetrexed.

DISCUSSION

In this study, we have investigated the effects of TS overexpression on the sensitivity of NSCLC cells to pemetrexed. Pemetrexed-resistant lung cancer cell lines established by stepwise exposure to increasing concentrations of pemetrexed were recently shown to contain increased amounts of TS mRNA compared with parental cells (Ozasa *et al*, 2010). Other previous studies have also found that sensitivity to pemetrexed is inversely related to the level of TS expression in cancer cell lines (Sigmond *et al*, 2003; Giovannetti *et al*, 2008). These observations have suggested that TS gene expression is associated with resistance to pemetrexed, but the

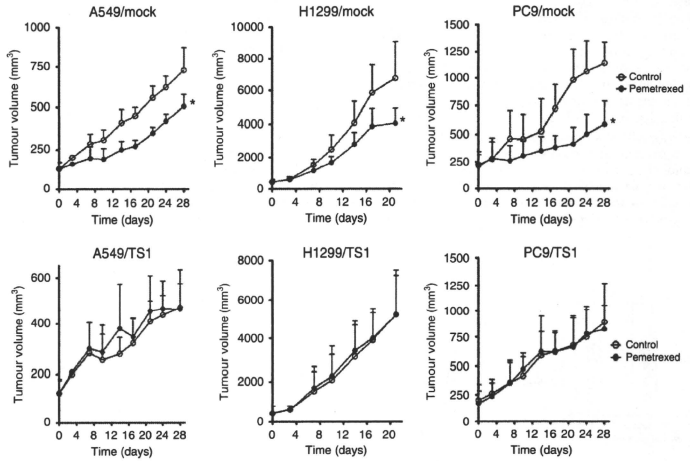

Figure 5 Effect of pemetrexed on the growth of TS-overexpressing NSCLC cells *in vivo*. Nude mice with tumour xenografts established by subcutaneous implantation of tumour fragments derived from the indicated NSCLC cell lines were treated with vehicle (control) or pemetrexed (100 mg kg^{-1}, intraperitoneal) on days 1, 8, 15, and 22. Tumour volume was determined at the indicated times after the onset of treatment. Data are means ± s.e.m. of values from eight mice per group. *$P<0.05$ for pemetrexed *vs* the corresponding value for vehicle (Student's two-tailed *t*-test).

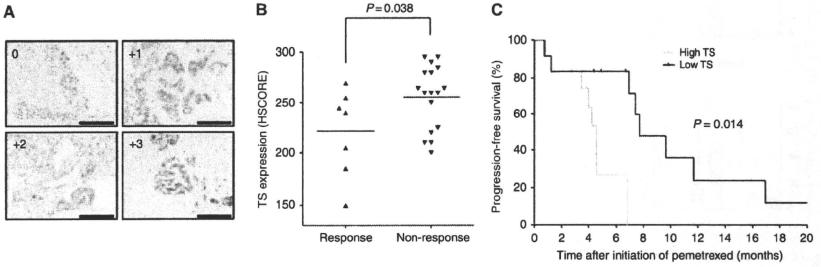

Figure 6 Relation of TS expression level to tumour response in NSCLC patients treated with pemetrexed and either carboplatin or cisplatin. (**A**) Representative sections of carcinomas including cells with the indicated intensities of TS immunostaining. Scale bars, 125 μm. (**B**) TS expression level (HSCORE) for the clinical specimens of 24 patients classified according to tumour response (response = CR or PR, $n = 7$; non-response = SD or PD, $n = 17$). Horizontal lines indicate mean values. The *P* value was determined by Student's two-tailed *t* test. (**C**) Progression-free survival of the NSCLC patients according to the expression level of TS in tumour specimens. The *P*-value was determined with the log-rank test.

Table 2 Patient characteristics

Characteristic	
Sex	
Male	17
Female	7
Mean (range) age (years)	66 (38–85)
Chemotherapy	
Carboplatin+pemetrexed	23
Cisplatin+pemetrexed	1
Tumor histology	
Adenocarcinoma	21
Squamous cell	1
Other	2
Disease stage	
IIIB	7
IV	17
Tumor response	
CR+PR	7
SD	13
PD	4

Abbreviations: CR = complete response; PD = progressive disease; PR = partial response; SD = stable disease.

mechanism by which a high level of TS expression might result in a reduced sensitivity to pemetrexed has remained unclear. Thymidylate synthase has a central role in the biosynthesis of thymidylate, an essential precursor for DNA synthesis (Carreras and Santi, 1995). We have previously shown that TS expression level differs among lung cancer cell lines, and that RNA interference-mediated depletion of TS in such cell lines resulted in growth suppression through inhibition of DNA synthesis and induction of apoptosis in a manner independent of the original level of TS activity (Takezawa *et al*, 2010). Pemetrexed exerts its cytotoxic effects through inhibition of multiple DNA synthesis-related enzymes including TS. We have now shown that pemetrexed inhibited DNA synthesis and induced apoptosis in NSCLC cell lines; however, it failed to induce such effects in the corresponding cells engineered to overexpress TS. Forced expression of TS also abolished the antitumour effect of pemetrexed in xenograft models. Our data suggest that pemetrexed did not fully inhibit TS activity in TS-overexpressing cells, given that DNA synthesis remained active after pemetrexed exposure. They further suggest that the observed reduction in the sensitivity of TS-overexpressing cells to pemetrexed may result from sustained activity of TS in the presence of the drug. We also examined the possible effect of pemetrexed on the expression levels of apoptosis-related molecules in both Mock and TS-overexpressing cells, but we found that pemetrexed did not substantially alter the abundance of such proteins including that of XIAP (data not shown), which we previously identified as having a key role in TS depletion-induced apoptosis in NSCLC cells (Takezawa *et al*, 2010). The precise mechanism by which pemetrexed induces apoptosis thus remains to be determined.

Previous studies have examined the possible relation between TS expression level and the response to pemetrexed in cancer patients (Gomez *et al*, 2006; Righi *et al*, 2010; Uramoto *et al*, 2010). In a phase II trial of pemetrexed monotherapy for advanced breast cancer (Gomez *et al*, 2006), 61 patients were treated with pemetrexed and evaluable for response. This study revealed a potential association between a high level of TS mRNA and a poor response to pemetrexed treatment. Another study evaluated TS expression level immunohistochemically by means of the HSCORE system in 60 patients with malignant mesothelioma treated either with the combination of pemetrexed and platinum, or with pemetrexed alone (Righi *et al*, 2010). A significant inverse correlation was found between TS expression level and time to progression, or overall survival. Finally, no significant correlation between the abundance of TS mRNA and clinical outcome was apparent for five NSCLC patients treated with the combination of pemetrexed and platinum, or with pemetrexed alone (Uramoto *et al*, 2010), although the small sample number precluded any definitive conclusion. In this study, we found that a high level of TS expression in human NSCLC tumours was significantly associated with a reduced tumour response and a shorter progression-free survival in 24 patients treated with pemetrexed combined with platinum agents, consistent with the previous studies of patients with breast cancer or malignant mesothelioma (Gomez *et al*, 2006; Righi *et al*, 2010). Given that the anticancer effects of cisplatin were independent of TS expression level in NSCLC cell lines, the relation between TS expression level and clinical outcome observed in our clinical analysis likely reflects the effect of pemetrexed. We recently evaluated the abundance of TS in NSCLC tumours of patients treated with carboplatin and paclitaxel, and neither a prognostic nor predictive role was identified for TS expression level in these patients (Takeda *et al*, 2010). Together with such observations, our present results suggest that assessment of baseline TS expression may be of predictive value in evaluation of chemosensitivity to pemetrexed in NSCLC. Although we cannot exclude a contribution of factors other than TS expression level to pemetrexed chemosensitivity, our preclinical and clinical data provide a rationale for the potential use of TS expression level as a predictive biomarker for response to pemetrexed or pemetrexed-based chemotherapy in patients with NSCLC. Further investigation is needed with a larger cohort of patients or in prospective studies to confirm this conclusion.

REFERENCES

Carreras CW, Santi DV (1995) The catalytic mechanism and structure of thymidylate synthase. *Annu Rev Biochem* **64:** 721–762

Ceppi P, Volante M, Saviozzi S, Rapa I, Novello S, Cambieri A, Lo Iacono M, Cappia S, Papotti M, Scagliotti GV (2006) Squamous cell carcinoma of the lung compared with other histotypes shows higher messenger RNA and protein levels for thymidylate synthase. *Cancer* **107:** 1589–1596

Ferguson PJ, Collins O, Dean NM, DeMoor J, Li CS, Vincent MD, Koropatnick J (1999) Antisense down-regulation of thymidylate synthase to suppress growth and enhance cytotoxicity of 5-FUdR, 5-FU and Tomudex in HeLa cells. *Br J Pharmacol* **127:** 1777–1786

Giovannetti E, Lemos C, Tekle C, Smid K, Nannizzi S, Rodriguez JA, Ricciardi S, Danesi R, Giaccone G, Peters GJ (2008) Molecular mechanisms underlying the synergistic interaction of erlotinib, an epidermal growth factor receptor tyrosine kinase inhibitor, with the multitargeted antifolate pemetrexed in non-small-cell lung cancer cells. *Mol Pharmacol* **73:** 1290–1300

Gomez HL, Santillana SL, Vallejos CS, Velarde R, Sanchez J, Wang X, Bauer NL, Hockett RD, Chen VJ, Niyikiza C, Hanauske AR (2006) A phase II trial of pemetrexed in advanced breast cancer: clinical response and association with molecular target expression. *Clin Cancer Res* **12:** 832–838

Hoffman PC, Mauer AM, Vokes EE (2000) Lung cancer. *Lancet* **355:** 479–485

Johnston PG, Fisher ER, Rockette HE, Fisher B, Wolmark N, Drake JC, Chabner BA, Allegra CJ (1994) The role of thymidylate synthase expression in prognosis and outcome of adjuvant chemotherapy in patients with rectal cancer. *J Clin Oncol* **12:** 2640–2647

Johnston PG, Mick R, Recant W, Behan KA, Dolan ME, Ratain MJ, Beckmann E, Weichselbaum RR, Allegra CJ, Vokes EE (1997) Thymidylate synthase expression and response to neoadjuvant

chemotherapy in patients with advanced head and neck cancer. *J Natl Cancer Inst* **89:** 308–313

Monica V, Scagliotti GV, Ceppi P, Righi L, Cambieri A, Lo Iacono M, Saviozzi S, Volante M, Novello S, Papotti M (2009) Differential thymidylate synthase expression in different variants of large-cell carcinoma of the lung. *Clin Cancer Res* **15:** 7547–7552

Okamoto W, Okamoto I, Tanaka K, Hatashita E, Yamada Y, Kuwata K, Yamaguchi H, Arao T, Nishio K, Fukuoka M, Janne PA, Nakagawa K (2010) TAK-701, a humanized monoclonal antibody to hepatocyte growth factor, reverses gefitinib resistance induced by tumor-derived HGF in non-small cell lung cancer with an EGFR mutation. *Mol Cancer Ther* **9:** 2785–2792

Ozasa H, Oguri T, Uemura T, Miyazaki M, Maeno K, Sato S, Ueda R (2010) Significance of thymidylate synthase for resistance to pemetrexed in lung cancer. *Cancer Sci* **101:** 161–166

Pestalozzi BC, Peterson HF, Gelber RD, Goldhirsch A, Gusterson BA, Trihia H, Lindtner J, Cortes-Funes H, Simmoncini E, Byrne MJ, Golouh R, Rudenstam CM, Castiglione-Gertsch M, Allegra CJ, Johnston PG (1997) Prognostic importance of thymidylate synthase expression in early breast cancer. *J Clin Oncol* **15:** 1923–1931

Righi L, Papotti MG, Ceppi P, Bille A, Bacillo E, Molinaro L, Ruffini E, Scagliotti GV, Selvaggi G (2010) Thymidylate synthase but not excision repair cross-complementation group 1 tumor expression predicts outcome in patients with malignant pleural mesothelioma treated with pemetrexed-based chemotherapy. *J Clin Oncol* **28:** 1534–1539

Scagliotti GV, Parikh P, von Pawel J, Biesma B, Vansteenkiste J, Manegold C, Serwatowski P, Gatzemeier U, Digumarti R, Zukin M, Lee JS, Mellemgaard A, Park K, Patil S, Rolski J, Goksel T, de Marinis F, Simms L, Sugarman KP, Gandara D (2008) Phase III study comparing cisplatin plus gemcitabine with cisplatin plus pemetrexed in chemotherapy-naive patients with advanced-stage non-small-cell lung cancer. *J Clin Oncol* **26:** 3543–3551

Schiller JH, Harrington D, Belani CP, Langer C, Sandler A, Krook J, Zhu J, Johnson DH (2002) Comparison of four chemotherapy regimens for advanced non-small-cell lung cancer. *N Engl J Med* **346:** 92–98

Shih C, Chen VJ, Gossett LS, Gates SB, MacKellar WC, Habeck LL, Shackelford KA, Mendelsohn LG, Soose DJ, Patel VF, Andis SL, Bewley JR, Rayl EA, Moroson BA, Beardsley GP, Kohler W, Ratnam M, Schultz RM (1997) LY231514, a pyrrolo[2,3-d]pyrimidine-based antifolate that inhibits multiple folate-requiring enzymes. *Cancer Res* **57:** 1116–1123

Sigmond J, Backus HH, Wouters D, Temmink OH, Jansen G, Peters GJ (2003) Induction of resistance to the multitargeted antifolate Pemetrexed (ALIMTA) in WiDr human colon cancer cells is associated with thymidylate synthase overexpression. *Biochem Pharmacol* **66:** 431–438

Takeda M, Okamoto I, Hirabayashi N, Kitano M, Nakagawa K (2010) Thymidylate synthase and dihydropyrimidine dehydrogenase expression levels are associated with response to S-1 plus carboplatin in advanced non-small cell lung cancer. *Lung Cancer*; doi:10.1016/j.lungcan.2010.10.022

Takezawa K, Okamoto I, Tsukioka S, Uchida J, Kiniwa M, Fukuoka M, Nakagawa K (2010) Identification of thymidylate synthase as a potential therapeutic target for lung cancer. *Br J Cancer* **103:** 354–361

Uramoto H, Onitsuka T, Shimokawa H, Hanagiri T (2010) TS, DHFR and GARFT expression in non-squamous cell carcinoma of NSCLC and malignant pleural mesothelioma patients treated with pemetrexed. *Anticancer Res* **30:** 4309–4315

Published OnlineFirst March 17, 2011; DOI:10.1158/1078-0432.CCR-10-2798

Clinical Cancer Research

Human Cancer Biology

Role of ERK-BIM and STAT3-Survivin Signaling Pathways in ALK Inhibitor–Induced Apoptosis in EML4-ALK–Positive Lung Cancer

Ken Takezawa[1], Isamu Okamoto[1], Kazuto Nishio[2], Pasi A. Jänne[3], and Kazuhiko Nakagawa[1]

Abstract

Purpose: *EML4-ALK* (echinoderm microtubule-associated protein–like 4 anaplastic lymphoma kinase) was recently identified as a transforming fusion gene in non–small cell lung cancer. The purpose of the present study was to characterize the mechanism of malignant transformation by EML4-ALK.

Experimental Design: We established NIH 3T3 cells that stably express variant 1 or 3 of EML4-ALK and examined the signaling molecules that function downstream of EML4-ALK.

Results: Forced expression of EML4-ALK induced marked activation of extracellular signal–regulated kinase (ERK) and STAT3, but not that of AKT. Inhibition of ERK or STAT3 signaling resulted in substantial attenuation of the proliferation of cells expressing either variant of EML4-ALK, suggesting that these signaling pathways function downstream of EML4-ALK in lung cancer cells. The specific ALK inhibitor TAE684 induced apoptosis that was accompanied both by upregulation of BIM, a proapoptotic member of the Bcl-2 family, and by downregulation of survivin, a member of the inhibitor of apoptosis protein (IAP) family, in EML4-ALK–expressing NIH 3T3 cells as well as in H3122 human lung cancer cells harboring endogenous EML4-ALK. Depletion of BIM and overexpression of survivin each inhibited TAE684-induced apoptosis, suggesting that both upregulation of BIM and downregulation of survivin contribute to TAE684-induced apoptosis in EML4-ALK–positive lung cancer cells. Furthermore, BIM and survivin expression was found to be independently regulated by ERK and STAT3 signaling pathways, respectively.

Conclusions: ALK inhibitor–induced apoptosis is mediated both by BIM upregulation resulting from inhibition of ERK signaling as well as by survivin downregulation resulting from inhibition of STAT3 signaling in EML4-ALK–positive lung cancer cells. *Clin Cancer Res; 17(8); 2140–8. ©2011 AACR.*

Introduction

Lung cancer is the leading cause of cancer deaths worldwide. Given that the efficacy of conventional chemotherapeutic agents with regard to improving clinical outcome in lung cancer patients is limited, target-based therapies are being pursued as potential treatment alternatives. Somatic mutations in the tyrosine kinase domain of the epidermal growth factor receptor (EGFR) have been associated with tumor responsiveness to EGFR tyrosine kinase inhibitors (TKI) in a subset of individuals with non–small cell lung cancer (NSCLC; refs. 1–3). Such findings suggest that the use of molecularly targeted therapy in genetically defined subsets of cancer patients may prove to be an effective strategy for the treatment of many cancers including NSCLC. Given that lung cancer is a common type of cancer, the identification of even small subsets of lung cancer patients harboring specific genetic abnormalities will translate into the provision of large cohorts for targeted therapy.

A recent study identified a potential driver mutation in NSCLC: fusion of the echinoderm microtubule-associated protein–like 4 gene (*EML4*) with the anaplastic lymphoma kinase gene (*ALK*), which results in the production of a fusion protein (EML4-ALK) consisting of the NH_2-terminal portion of EML4 and the COOH-terminal region of ALK (4). ALK was originally discovered as the result of characterization of chromosomal translocations that lead to the expression of fusion proteins consisting of the COOH-terminal kinase domain of ALK and the NH_2-terminal portion of nucleophosmin (NPM) in patients with anaplastic large cell lymphoma (5, 6). Various break and fusion points within the *EML4* locus in NSCLC cells give rise to different isoforms of EML4-ALK, which appear to be present in 5% to 10% of NSCLC cases (4, 7–14). The most common EML4-ALK variants are 1 and 3, which together account for about 60% of EML4-ALK–positive lung cancer cases (14). All EML4-ALK isoforms undergo constitutive oligomerization mediated by the coiled coil domain of the

Authors' Affiliations: Departments of [1]Medical Oncology and [2]Genome Biology, Kinki University Faculty of Medicine, Osaka, Japan; and [3]Lowe Center for Thoracic Oncology and Department of Medical Oncology, Dana-Farber Cancer Institute, Boston, Massachusetts

Note: Supplementary data for this article are available at Clinical Cancer Research Online (http://clincancerres.aacrjournals.org/).

Corresponding Author: Isamu Okamoto, Department of Medical Oncology, Kinki University Faculty of Medicine, 377-2 Ohno-higashi, Osaka-Sayama, Osaka 589-8511, Japan. Phone: 81-72-366-0221; Fax: 81-72-360-5000; E-mail: chi-okamoto@dotd.med.kindai.ac.jp

doi: 10.1158/1078-0432.CCR-10-2798

Published OnlineFirst March 17, 2011; DOI:10.1158/1078-0432.CCR-10-2798

Translational Relevance

EML4-ALK (echinoderm microtubule-associated protein–like 4 anaplastic lymphoma kinase) was recently identified as a transforming fusion gene in non–small cell lung cancer (NSCLC), and several selective inhibitors of the kinase activity of ALK, such as crizotinib, are currently undergoing clinical trials for the treatment of EML4-ALK–positive NSCLC. Identification of the signaling pathways responsible for malignant transformation by EML4-ALK will likely enhance further development of ALK-targeted therapy for NSCLC patients. We have now shown that both ERK (extracellular signal–regulated kinase) and STAT3 pathways are the principal mediators of EML4-ALK signaling, and we further identified the mediators of apoptosis induced by ALK inhibition. Our preclinical data provide both insight into the pathogenesis of EML4-ALK–positive lung cancer and a potential basis for the development of biomarkers for the efficacy of ALK-targeted therapy in patients with this condition.

EML4 portion, which confers marked transforming activity both *in vitro* and *in vivo* (4, 15).

ALK inhibitors have been found to suppress the growth of and to induce apoptosis in EML4-ALK–positive lung cancer cells, suggesting that ALK inhibition is a potential strategy for the treatment of NSCLC patients with this molecular abnormality (9, 16). Indeed, a selective inhibitor of the kinase activity of ALK, crizotinib, is currently undergoing clinical trials and has shown high efficacy in NSCLC patients with EML4-ALK (17). However, the downstream signaling pathways that regulate the proliferation or survival of EML4-ALK–positive lung cancer cells have remained to be well established, and the key mediators of ALK inhibitor–induced apoptosis have not been fully determined. In the present study, we constructed expression vectors for EML4-ALK variants 1 and 3 and then established cells stably expressing these proteins. With the use of these cells, we examined the signaling molecules that function downstream of EML4-ALK. We further investigated the molecular mechanisms underlying ALK inhibitor–induced apoptosis in EML4-ALK–positive lung cancer cells.

Materials and Methods

Cell culture and reagents

NIH 3T3 cells as well as the human cancer cell lines H2228 and Karpas299 were obtained from American Type Culture Collection. H3122 cells were obtained as previously described (9). NIH 3T3 cells were cultured in Dulbecco's modified Eagle's medium (Sigma) supplemented with 10% FBS and 1% penicillin-streptomycin. H2228, Karpas299, and H3122 cells were cultured in RPMI 1640 medium (Sigma) supplemented with 10% FBS and 1% penicillin-streptomycin. All cells were maintained under a humidified atmosphere of 5% CO_2 at 37°C. U0126 and LY294002 were obtained from Cell Signaling Technology and TAE684 was from ShangHai Biochempartner.

Cell transfection

A cDNA for EML4-ALK variant 1 was cloned into pDNR-Dual (Becton Dickinson) as previously described (9). A full-length cDNA fragment encoding EML4-ALK variant 3b was obtained from H2228 cells by reverse transcription and the PCR with the primers EAV-F (5′-AAGCTTCGCAAGATGGACGGTTTCGCCGGCAGTC-3′) and EAV-R (5′-GCGGCCGCTCAGGGCCCAGGC-TGGTTCATGCT-3′). Amplification products were verified by sequencing after their cloning into the pCR-Blunt II-TOPO vector (Invitrogen). The EML4-ALK variant 1 or 3b cDNA was excised from pCR-Blunt II-TOPO and transferred to either pcDNA3.1-Hygro(+) (Invitrogen) or pMZs (Cell Biolabs). A pBabe-puro vector encoding CA-STAT3 with a COOH-terminal FLAG tag was kindly provided by J. Bromberg (18). A pQCXIH-survivin vector was constructed as previously described (19). All expression vectors were introduced into NIH 3T3 cells as previously described (20, 21).

Immunoblot analysis

Cells were washed twice with ice-cold PBS and then lysed in a solution containing 20 mmol/L Tris-HCl (pH 7.5), 150 mmol/L NaCl, 1 mmol/L EDTA, 1% Triton X-100, 2.5 mmol/L sodium pyrophosphate, 1 mmol/L phenylmethylsulfonyl fluoride, and leupeptin (1 μg/mL). The protein concentration of cell lysates was determined with the Bradford reagent (Bio-Rad), and equal amounts of protein were subjected to SDS-PAGE on a 7.5% or 12% gel. The separated proteins were transferred to a nitrocellulose membrane, which was then exposed to 5% nonfat dried milk in PBS for 1 hour at room temperature before incubation overnight at 4°C with primary antibodies. Rabbit polyclonal antibodies to human phosphorylated ALK (pY1608), to ALK, to phosphorylated extracellular signal–regulated kinase (ERK), to ERK, to phosphorylated STAT3, to STAT3, to phosphorylated AKT, to AKT, to PARP, to BIM, to Mcl-1, to Bcl-xL, to X-linked inhibitor of apoptosis (XIAP), and to FLAG were obtained from Cell Signaling Technology; those to survivin were from Novos; and those to β-actin were from Sigma. All antibodies were used at a 1:1,000 dilution, with the exception of those to β-actin (1:200). The membrane was then washed with PBS containing 0.05% Tween 20 before incubation for 1 hour at room temperature with horseradish peroxidase–conjugated goat antibodies to rabbit IgG (Sigma). Immune complexes were finally detected with chemiluminescence reagents (GE Healthcare).

Cell growth inhibition assay

Cells were plated in 96-well, flat-bottomed plates and cultured for 24 hours before exposure to various concentrations of drugs for 72 hours. TetraColor One (5 mmol/L tetrazolium monosodium salt and 0.2 mmol/L 1-methoxy-5-methyl phenazinium methylsulfate; Seikagaku) was then

Published OnlineFirst March 17, 2011; DOI:10.1158/1078-0432.CCR-10-2798

added to each well, and the cells were incubated for 3 hours at 37°C before measurement of absorbance at 490 nm with a Multiskan Spectrum instrument (Thermo Labsystems).

RNA interference

Cells were plated at 50% to 60% confluence in 6-well plates or 25-cm^2 flasks and then incubated for 24 hours before transient transfection for the indicated times with siRNAs mixed with the Lipofectamine reagent (Invitrogen). The siRNAs specific for STAT3 mRNA (STAT3-1, 5′-UCAUUGACCUUGUGAAAAA-3′; STAT3-2, 5′-GCAAAAA-GUUUCCUACAAA-3′), ALK mRNA (ALK-1, 5′-ACACC-CAAAUUAAUACCAA-3′; ALK-2, 5′-UCAGCAAAUUCAA-CCACCA-3′), ERK mRNA (ERK-1, 5′-CAAGAGGAUUGAA-GUAGAA-3′; ERK-2, 5′-UCAGCCCCUUUGAGCACCA-3′), or BIM mRNA (BIM-1, 5′-GGAGGGUAUUUUUGAAUAA-3′; BIM-2, 5′-AGGAGGGUAUUUUUGAAUA-3′) as well as a nonspecific siRNA (5′-GUUGAGAGAUAUUAGAGUU-3′) were obtained from Nippon EGT. The cells were then subjected to immunoblot analysis or the annexin V–binding assay. All data presented were obtained with STAT3-1, ALK-1, ERK-1, or BIM-1 siRNAs, but similar results were obtained with STAT3-2, ALK-2, ERK-2, and BIM-2 siRNAs.

Annexin V–binding assay

Binding of annexin V to cells was measured with the use of an Annexin-V-FLUOS Staining kit (Roche). Cells were harvested by exposure to trypsin-EDTA, washed with PBS, and centrifuged at 200 × *g* for 5 minutes. The cell pellets were resuspended in 100 μL of Annexin-V-FLUOS labeling solution, incubated for 10 to 15 minutes at 15°C to 25°C, and then analyzed for fluorescence with a flow cytometer (FACSCalibur) and Cell Quest software (Becton Dickinson).

Statistical analysis

Quantitative data are presented as means ± SD and were analyzed by Student's 2-tailed *t* test. A value of $P < 0.05$ was considered statistically significant.

Results

Oncogenic EML4-ALK tyrosine kinase activates ERK and STAT3 signaling pathways

To study the function of oncogenic EML4-ALK, we established nontransformed mouse fibroblast (NIH 3T3) cells that either stably express EML4-ALK variant 1 or 3 (3T3/EAV1 and 3T3/EAV3 cells, respectively) or stably harbor the corresponding empty vector (3T3-Mock cells). Immunoblot analysis revealed that EML4-ALK variant 1 or 3 was detected with antibodies to ALK at positions corresponding to molecular sizes of about 120 and 90 kDa, respectively, in the transfected cells (Fig. 1A). The kinase activity of the EML4-ALK variants was activated as revealed by immunoblot

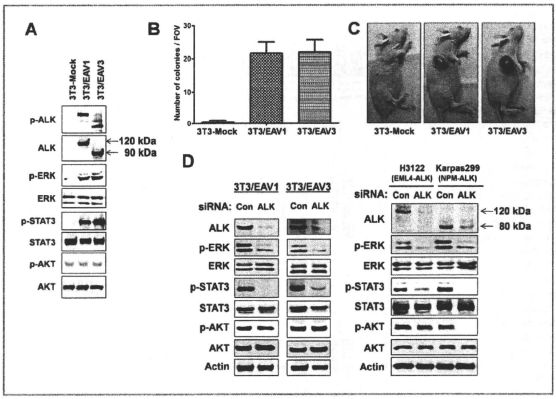

Figure 1. Effects of stable forced expression of EML4-ALK variant 1 or 3 on signaling pathways. A, the indicated stably transfected NIH 3T3 cell lines were lysed and subjected to immunoblot analysis with antibodies to the indicated proteins. B, the indicated cell lines were plated in semisolid medium supplemented with 10% FBS and incubated for 3 to 4 weeks, after which the cells were stained with 0.005% crystal violet and the number of colonies per field of view (FOV) was counted. Data are means ± SD from 3 independent experiments. C, cells (5×10^6) of the indicated lines were injected subcutaneously into the axilla of 5-week-old female athymic nude mice. At 18 days after the injection, the large tumors that formed at the injection site for 3T3/EAV1 or 3T3/EAV3 cells were photographed. Data are representative of results obtained with 5 mice per cell line. D, the indicated cell lines were transfected with nonspecific (Con) or ALK siRNAs for 48 hours, after which cell lysates were subjected to immunoblot analysis with antibodies to the indicated proteins.

Published OnlineFirst March 17, 2011; DOI:10.1158/1078-0432.CCR-10-2798

analysis with antibodies specific for the Tyr^{1608}-phosphorylated form of ALK. Consistent with previous observations (4, 15), the 3T3/EAV cells exhibited transforming activity both *in vitro* (Fig. 1B) and *in vivo* (Fig. 1C). We also found that phosphorylation of both the mitogen-activated protein kinase (MAPK) ERK and STAT3 was markedly increased in the cells expressing either variant of EML4-ALK compared with that in 3T3-Mock cells, whereas the phosphorylation level of the kinase AKT was not affected by expression of EML4-ALK (Fig. 1A). To exclude the possibility that these results were due to nonspecific effects of transfection, we depleted both 3T3/EAV1 and 3T3/EAV3 cells of EML4-ALK by RNA interference (RNAi) with ALK siRNA. The phosphorylation of both ERK and STAT3, but not that of AKT, was markedly suppressed by depletion of EML4-ALK (Fig. 1D). Moreover, similar depletion of endogenous EML4-ALK variant 1 in the lung cancer cell line H3122 resulted in marked inhibition of the phosphorylation of ERK and STAT3 without an effect on that of AKT (Fig. 1D). In contrast, the phosphorylation of ERK, STAT3, and AKT was inhibited by ALK siRNA in the NPM-ALK–positive lymphoma cell line Karpas299 (Fig. 1D), in which activation of the phosphoinositide 3-kinase (PI3K)-AKT signaling pathway has been shown to contribute to malignant transformation (22–25). Together, these data suggested that either variant 1 or 3 of EML4-ALK activates ERK and STAT3 signaling pathways but not the PI3K-AKT signaling pathway.

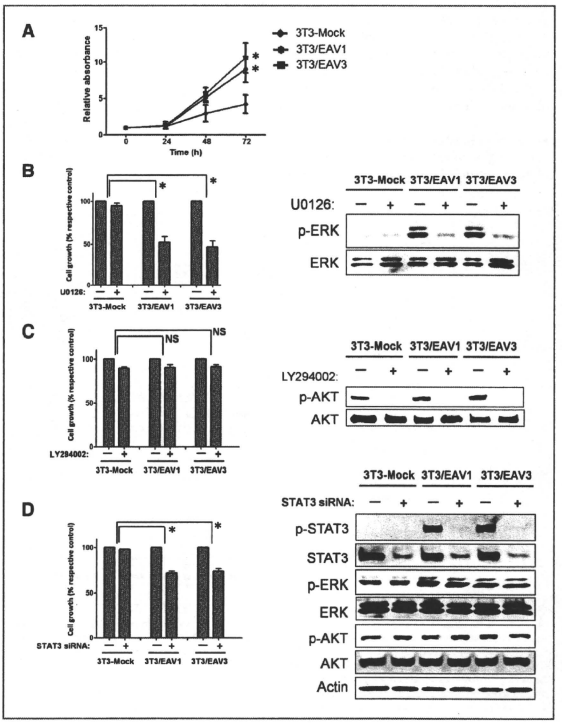

Figure 2. Effects of inhibition of ERK, PI3K, or STAT3 signaling on the growth of cells expressing EML4-ALK. A, the indicated cell lines were incubated in complete medium for the indicated times, after which cell viability was assessed as described in the "Materials and Methods" section. Data are expressed relative to the absorbance value for 3T3-Mock cells at time 0. B and C, cells were incubated in complete medium with or without 10 μmol/L U0126 (B) or 10 μmol/L LY294002 (C) for 72 or 24 hours, after which cell viability was assessed (left) or cell lysates were subjected to immunoblot analysis with antibodies to the indicated proteins (right), respectively. D, cells were transfected with nonspecific or STAT3 siRNAs for 72 or 48 hours, after which cell viability was assessed (left) or cell lysates were subjected to immunoblot analysis with antibodies to the indicated proteins (right), respectively. The abundance of β-actin was examined as a loading control. All quantitative data are means ± SD from 3 independent experiments. *, $P < 0.05$ versus the corresponding value for 3T3-Mock cells or for the indicated comparisons. NS, not significant.

Published OnlineFirst March 17, 2011; DOI:10.1158/1078-0432.CCR-10-2798

EML4-ALK promotes cell proliferation through ERK and STAT3 signaling pathways

We next examined the effect of EML4-ALK on cell proliferation. Both 3T3/EAV1 and 3T3/EAV3 cells proliferated significantly faster than did 3T3-Mock cells (Fig. 2A). To determine the role of intracellular signaling pathways in this action of EML4-ALK, we first examined the effects of chemical inhibitors. We found that UI0126, an inhibitor of the ERK kinase MEK, had little effect on the growth of 3T3-Mock cells but that it significantly inhibited the proliferation of both 3T3/EAV1 and 3T3/EAV3 cells at a concentration (10 μmol/L) that resulted in marked inhibition of ERK phosphorylation (Fig. 2B). These data thus suggested that the MEK-ERK signaling pathway contributes to the regulation of cell proliferation by EML4-ALK. We also found that the specific PI3K inhibitor LY294002 had no significant effect on the growth of 3T3-Mock cells or on that of 3T3/EAV1 and 3T3/EAV3 cells at a concentration (10 μmol/L) at which the phosphorylation of AKT was largely abolished (Fig. 2C). To examine the effect of STAT3 inhibition on cell proliferation in cells expressing EML4-ALK, we transfected the cells with an siRNA specific for STAT3 mRNA. Transfection of 3T3-Mock, 3T3/EAV1, or 3T3/EAV3 cells with STAT3 siRNA resulted in marked depletion of STAT3 (Fig. 2D). Whereas such depletion of STAT3 did not affect the proliferation of 3T3-Mock cells, it significantly inhibited that of 3T3/EAV1 and 3T3/EAV3 cells (Fig. 2D). A

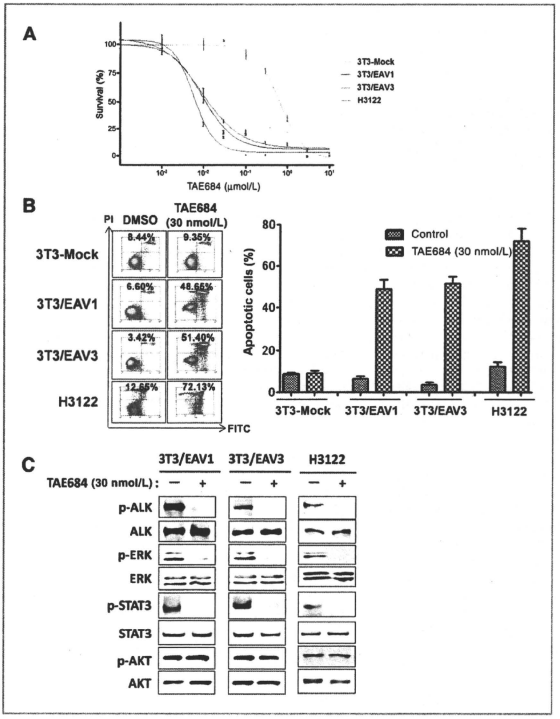

Figure 3. Effects of TAE684 on cell growth, apoptosis, and intracellular signaling in cells expressing EML4-ALK. A, the indicated cell lines were cultured for 72 hours in complete medium containing various concentrations of TAE684, after which cell viability was assessed. Data are expressed as percent survival and are means ± SD of triplicates from an experiment that was repeated a total of 3 times with similar results. B, cells were incubated for 48 hours in serum-free medium with 30 nmol/L TAE684 or 0.01% dimethyl sulfoxide (DMSO, vehicle control), after which the proportion of apoptotic cells was determined by staining with fluorescein isothiocyanate (FITC)-conjugated annexin V and propidium iodide (PI) followed by flow cytometry. Representative flow cytometric profiles, with the percentages of FITC-positive, PI-negative (apoptotic) cells indicated, are shown in the left. Quantitative data in the right are means ± SD of triplicates from an experiment that was repeated a total of 3 times with similar results. C, cells were incubated for 24 hours in serum-free medium with or without 30 nmol/L TAE684, after which cell lysates were subjected to immunoblot analysis with antibodies to the indicated proteins.

Published OnlineFirst March 17, 2011; DOI:10.1158/1078-0432.CCR-10-2798

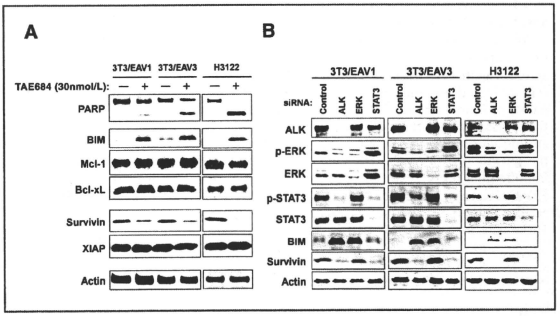

Figure 4. Effects of TAE684 on the expression of apoptosis-related proteins in cells expressing EML4-ALK. A, the indicated cell lines were incubated for 48 hours in serum-free medium with or without 30 nmol/L TAE684, after which cell lysates were subjected to immunoblot analysis with antibodies to the indicated proteins. B, 3T3/EAV1, 3T3/EAV3, or H3122 cells were transfected with nonspecific (control), ALK, ERK, or STAT3 siRNAs for 48 hours, after which cell lysates were subjected to immunoblot analysis with antibodies to the indicated proteins.

second siRNA targeted to a different region of STAT3 mRNA yielded similar results (data not shown). These observations thus suggested that EML4-ALK promotes cell proliferation through both MEK-ERK and STAT3 signaling pathways but not through the PI3K-AKT signaling pathway.

Effects of ALK inhibition on cell growth and intracellular signaling in EML4-ALK–positive lung cancer cells

To investigate the effects of inhibition of the kinase activity of ALK on cell growth and intracellular signaling in cells expressing EML4-ALK, we used TAE684, a selective and highly potent ALK inhibitor (26). The human lung cancer cell line H3122 expresses endogenous EML4-ALK variant 1 and its growth was found to be highly sensitive to TAE684 (Fig. 3A). Treatment with TAE684 also induced a large increase in the number of apoptotic H3122 cells, as revealed with an annexin V–binding assay (Fig. 3B). Consistent with these results, both 3T3/EAV1 and 3T3/EAV3 cells exhibited a sensitivity to TAE684 that was about 100 times as great as that of 3T3-Mock cells (Fig. 3A), and the level of apoptosis induced by this drug was markedly greater in both 3T3/EAV1 and 3T3/EAV3 cells than in 3T3-Mock cells (Fig. 3B). Immunoblot analysis revealed that TAE684 inhibited the phosphorylation of EML4-ALK in 3T3/EAV1, 3T3/EAV3, and H3122 cells at a concentration (30 nmol/L) at which it substantially inhibited the growth of these cells (Fig. 3C). We further found that TAE684 inhibited the activation of ERK and STAT3, without affecting that of AKT, in all 3 of these cell lines (Fig. 3C). These data thus suggested that the ALK inhibitor induced growth suppression and apoptosis in EML4-ALK–positive lung cancer cells, and that these effects were accompanied by inhibition of ERK and STAT3 signaling pathways but not by that of the PI3K-AKT signaling pathway.

Effects of ALK inhibition on the expression of apoptosis-related proteins in EML4-ALK–positive lung cancer cells

Given that TAE684 induced apoptosis in cells expressing EML4-ALK, we examined the effects of this drug on the expression of apoptosis-related proteins in such cells. TAE684 induced cleavage of PARP, a characteristic of apoptosis, in H3122 cells as well as in 3T3/EAV1 and 3T3/EAV3 cells (Fig. 4A). TAE684 also increased the abundance of BIM, a proapoptotic member of the Bcl-2 family of proteins, in cells expressing EML4-ALK, whereas the amounts of the Bcl-2 family members Mcl-1 and Bcl-xL remained unaffected (Fig. 4A). In contrast, TAE684 induced downregulation of the expression of survivin, a member of the IAP family, in cells expressing EML4-ALK, whereas the expression of XIAP, another IAP family member, remained unaffected (Fig. 4A). To investigate the possible roles of the ERK and STAT3 signaling pathways in the induction of BIM and downregulation of survivin by TAE684, we examined the effects of EML4-ALK, ERK, or STAT3 depletion by RNAi in 3T3/EAV1, 3T3/EAV3, and H3122 cells. Similar to the effects of TAE684 (Fig. 3C), depletion of EML4-ALK with an ALK siRNA resulted in inhibition of both ERK and STAT3 phosphorylation in all 3 cell lines (Fig. 4B). The amount of BIM was increased as a result of EML4-ALK or ERK depletion but was not affected by STAT3 depletion (Fig. 4B). In contrast, the expression of survivin was inhibited by depletion of EML4-AKT or STAT3 but not by that of ERK (Fig. 4B). Similar results were obtained with a second set of ALK, ERK, and STAT3 siRNAs targeted to different regions of the corresponding mRNAs (data not shown). These data thus suggested that ALK inhibition results in upregulation of BIM expression through inhibition of the ERK signaling pathway as well as in downregulation of survivin expression through inhibition of the STAT3 signaling pathway.

Published OnlineFirst March 17, 2011; DOI:10.1158/1078-0432.CCR-10-2798

Role of ERK-BIM and STAT3-survivin signaling pathways in TAE684-induced apoptosis in cells expressing EML4-ALK

To investigate further whether induction of BIM is related to TAE684-induced apoptosis, we transfected 3T3/EAV3 or H3122 cells with an siRNA specific for BIM mRNA. Such transfection largely blocked BIM induction by TAE684 (Fig. 5A). Staining with annexin V revealed that RNAi-mediated attenuation of BIM induction resulted in significant inhibition of TAE684-induced apoptosis in both cell lines (Fig. 5A), implicating upregulation of BIM expression in the induction of apoptosis by TAE684 in EML4-ALK–positive cells. We obtained similar results with a second siRNA targeted to a different sequence within BIM mRNA (data not shown). Given that TAE684 inhibited STAT3-survivin signaling in cells expressing EML4-ALK, we next investigated the contribution of such signaling to TAE684-induced apoptosis by transfecting 3T3/EAV3 or H3122 cells with an expression vector encoding a FLAG epitope–tagged constitutively active (CA) form of human STAT3. Expression of CA-STAT3 increased the abundance of survivin (Fig. 5B), consistent with the notion that survivin expression is upregulated by activation of STAT3 signaling. Furthermore, expression of CA-STAT3 inhibited the downregulation of survivin induced by TAE684, without affecting BIM induction (Fig. 5B), and it significantly inhibited TAE684-induced apoptosis (Fig. 5B). These data suggested that inhibition of the STAT3 signaling pathway contributes to TAE684-induced apoptosis in EML4-ALK–positive cells. To confirm that TAE684-induced apoptosis mediated by STAT3 inhibition was attributable to downregulation of survivin expression, we transfected 3T3/EAV3 or H3122 cells with an expression vector for human survivin. Survivin overexpression resulted in substantial inhibition of the TAE684-induced downregulation of survivin in both 3T3/EAV3 and H3122 cells (Fig. 5C), and this effect was associated with significant inhibition

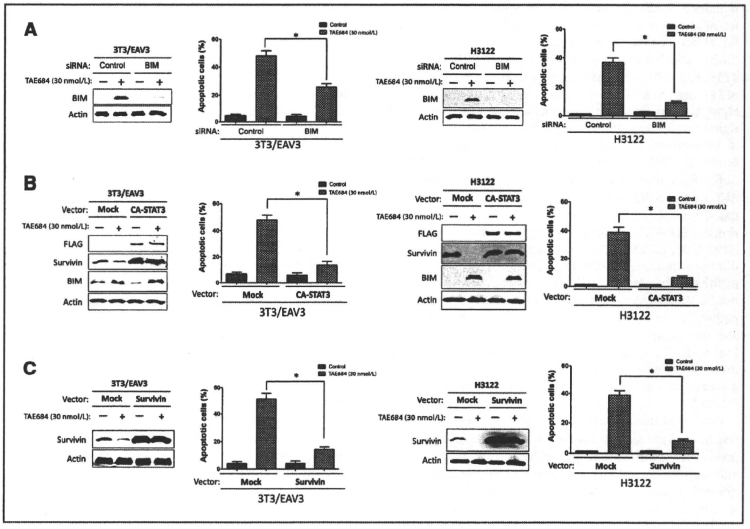

Figure 5. Effects of BIM depletion as well as forced expression of CA-STAT3 and survivin on apoptosis induced by TAE684 in 3T3/EAV3 or H3122 cells. A, cells were transfected with nonspecific (control) or BIM siRNAs for 24 hours and then incubated in complete medium with 30 nmol/L TAE684 or DMSO vehicle for 48 hours, after which cells either were lysed and subjected to immunoblot analysis with antibodies to the indicated proteins or were evaluated for apoptosis by staining with annexin V and PI followed by flow cytometry. B, cells were transfected with an expression vector for FLAG-tagged CA-STAT3 or with the corresponding empty vector for 24 hours and were then incubated with or without 30 nmol/L TAE684 for 48 hours and analyzed as in A. C, cells were transfected with an expression vector for survivin or with the corresponding empty vector for 24 hours and were then incubated with or without 30 nmol/L TAE684 for 48 hours and analyzed as in A. All quantitative data are means ± SD from at least 3 independent experiments. *, $P < 0.05$ for the indicated comparisons.

Published OnlineFirst March 17, 2011; DOI:10.1158/1078-0432.CCR-10-2798

of TAE684-induced apoptosis (Fig. 5C). These results thus suggested that inhibition of STAT3-survivin signaling by TAE684 contributes substantially to the induction of apoptosis by this drug. Collectively, our results thus suggested that inhibition of both the ERK-BIM and STAT3-survivin signaling pathways contributes to the induction of apoptosis associated with ALK inhibition in EML4-ALK–positive lung cancer cells.

Discussion

EML4-ALK was only recently identified as a transforming fusion gene in NSCLC (4). Although EML4-ALK was shown to possess marked oncogenic activity both *in vitro* and *in vivo* (4, 15), the signaling pathways underlying malignant transformation by the fusion protein have remained unclear. We have now shown that phosphorylation of both ERK and STAT3 was similarly and markedly increased in NIH 3T3 cells by forced expression of either variant 1 or variant 3 of EML4-ALK, whereas phosphorylation of AKT remained unaffected. Similar effects were observed in different clones of these cells stably transfected with a vector for either variant of EML4-ALK (data not shown). We further showed that the growth of both 3T3/EAV1 and 3T3/EAV3 cells was significantly attenuated by inhibition of ERK or STAT3 signaling but not by that of PI3K signaling. NPM-ALK has also been shown to activate ERK and STAT3 signaling pathways (6, 27–33), both of which are thought to be essential downstream mediators of the oncogenic action of NPM-ALK. In the present study, we found that ALK siRNA markedly abrogated the phosphorylation of AKT in the NPM-ALK–positive lymphoma cell line Karpas299, consistent with previous results implicating activation of PI3K-AKT signaling in malignant transformation by NPM-ALK (22–25). In contrast, we found that ALK siRNA did not suppress AKT phosphorylation in the EML4-ALK–positive lung cancer cell line H3122. Together, our results thus suggest that both ERK and STAT3 signaling pathways, rather than the PI3K signaling pathway, are the principal downstream pathways activated by EML4-ALK in lung cancer cells. Oncogenic ALK fusion proteins therefore may activate downstream pathways in a manner dependent on the fusion partner (Supplementary Fig. S1).

Preclinical studies have shown that treatment of NSCLC cell lines expressing EML4-ALK with ALK inhibitors suppresses cell proliferation and induces apoptosis (9, 34), although the underlying mechanisms of these effects were not well characterized. We have now shown that TAE684, a specific inhibitor of the kinase activity of ALK, significantly inhibited the phosphorylation of ERK and STAT3, but not that of AKT, in EML4-ALK–positive lung cancer cells, supporting the notion that ERK and STAT3 signaling pathways function downstream of EML4-ALK. BIM is a key proapoptotic member of the Bcl-2 family of proteins and initiates apoptosis signaling by binding to and antagonizing the function of prosurvival members of the Bcl-2 family (35). We found that TAE684 induced upregulation of BIM in EML4-ALK–positive lung cancer cells. With the use of RNAi-mediated depletion of ERK, we also found that BIM expression is regulated by the ERK signaling pathway. We further showed that knockdown of BIM by RNAi resulted in significant inhibition of TAE684-induced apoptosis in EML4-ALK–positive cells, suggesting that BIM induction mediated by inhibition of the ERK pathway plays a pivotal role in ALK inhibitor–induced apoptosis in EML4-ALK–positive lung cancer cells. These findings are consistent with the previous observation that inhibition of the ERK pathway contributes to EGFR-TKI–induced BIM upregulation, which is essential for the induction of apoptosis by these agents, in *EGFR* mutation–positive NSCLC cells (36–38).

Survivin is a member of the IAP family and protects against apoptosis by either directly or indirectly inhibiting the activation of effector caspases (39). We have now shown that TAE684 inhibited the expression of survivin in EML4-ALK–positive lung cancer cells. Furthermore, depletion of STAT3 resulted in downregulation of survivin expression, whereas expression of a constitutively active form of STAT3 resulted in upregulation of survivin expression. These data indicate that expression of survivin is regulated primarily through the STAT3 signaling pathway, consistent with the results of a previous study (40). We further found that expression of CA-STAT3 blocked the TAE684-induced downregulation of survivin, indicating that ALK inhibition results in survivin downregulation through inhibition of the STAT3 signaling pathway. Forced expression of either CA-STAT3 or survivin attenuated TAE684-induced apoptosis in 3T3/EAV3 or H3122 cells, suggesting that inhibition of STAT3-survivin signaling contributes to ALK inhibitor–induced apoptosis in EML4-ALK–positive lung cancer cells. Our present data thus suggest that ALK inhibitor–induced apoptosis is mediated both by upregulation of BIM through inhibition of the ERK pathway and by downregulation of survivin through inhibition of the STAT3 pathway in EML4-ALK–positive lung cancer cells.

In conclusion, our results have identified both ERK and STAT3 signaling pathways as key mediators of the transforming activity of EML4-ALK in lung cancer cells positive for this fusion protein. We further demonstrated that inhibition of both ERK-BIM and STAT3-survivin signaling pathways is responsible for ALK inhibitor–induced apoptosis in these cells. Our results thus provide a basis for the further development of ALK-targeted therapy in EML4-ALK–positive lung cancer patients.

Disclosure of Potential Conflicts of Interest

No potential conflicts of interest were disclosed.

The costs of publication of this article were defrayed in part by the payment of page charges. This article must therefore be hereby marked *advertisement* in accordance with 18 U.S.C. Section 1734 solely to indicate this fact.

Received October 19, 2010; revised January 20, 2011; accepted February 10, 2011; published OnlineFirst March 17, 2011.

Published OnlineFirst March 17, 2011; DOI:10.1158/1078-0432.CCR-10-2798

References

1. Lynch TJ, Bell DW, Sordella R, Gurubhagavatula S, Okimoto RA, Brannigan BW, et al. Activating mutations in the epidermal growth factor receptor underlying responsiveness of non-small-cell lung cancer to gefitinib. N Engl J Med 2004;350:2129–39.
2. Paez JG, Janne PA, Lee JC, Tracy S, Greulich H, Gabriel S, et al. EGFR mutations in lung cancer: correlation with clinical response to gefitinib therapy. Science 2004;304:1497–500.
3. Pao W, Miller V, Zakowski M, Doherty J, Politi K, Sarkaria I, et al. EGF receptor gene mutations are common in lung cancers from "never smokers" and are associated with sensitivity of tumors to gefitinib and erlotinib. Proc Natl Acad Sci U S A 2004;101:13306–11.
4. Soda M, Choi YL, Enomoto M, Takada S, Yamashita Y, Ishikawa S, et al. Identification of the transforming EML4-ALK fusion gene in non-small-cell lung cancer. Nature 2007;448:561–6.
5. Morris SW, Kirstein MN, Valentine MB, Dittmer KG, Shapiro DN, Saltman DL, et al. Fusion of a kinase gene, ALK, to a nucleolar protein gene, NPM, in non-Hodgkin's lymphoma. Science 1994;263:1281–4.
6. Fujimoto J, Shiota M, Iwahara T, Seki N, Satoh H, Mori S, et al. Characterization of the transforming activity of p80, a hyperphosphorylated protein in a Ki-1 lymphoma cell line with chromosomal translocation t(2;5). Proc Natl Acad Sci U S A 1996;93:4181–6.
7. Inamura K, Takeuchi K, Togashi Y, Nomura K, Ninomiya H, Okui M, et al. EML4-ALK fusion is linked to histological characteristics in a subset of lung cancers. J Thorac Oncol 2008;3:13–7.
8. Inamura K, Takeuchi K, Togashi Y, Hatano S, Ninomiya H, Motoi N, et al. EML4-ALK lung cancers are characterized by rare other mutations, a TTF-1 cell lineage, an acinar histology, and young onset. Mod Pathol 2009;22:508–15.
9. Koivunen JP, Mermel C, Zejnullahu K, Murphy C, Lifshits E, Holmes AJ, et al. EML4-ALK fusion gene and efficacy of an ALK kinase inhibitor in lung cancer. Clin Cancer Res 2008;14:4275–83.
10. Shinmura K, Kageyama S, Tao H, Bunai T, Suzuki M, Kamo T, et al. EML4-ALK fusion transcripts, but no NPM-, TPM3-, CLTC-, ATIC-, or TFG-ALK fusion transcripts, in non-small cell lung carcinomas. Lung Cancer 2008;61:163–9.
11. Martelli MP, Sozzi G, Hernandez L, Pettirossi V, Navarro A, Conte D, et al. EML4-ALK rearrangement in non-small cell lung cancer and non-tumor lung tissues. Am J Pathol 2009;174:661–70.
12. Shaw AT, Yeap BY, Mino-Kenudson M, Digumarthy SR, Costa DB, Heist RS, et al. Clinical features and outcome of patients with non-small-cell lung cancer who harbor EML4-ALK. J Clin Oncol 2009;27:4247–53.
13. Wong DW, Leung EL, So KK, Tam IY, Sihoe AD, Cheng LC, et al. The EML4-ALK fusion gene is involved in various histologic types of lung cancers from nonsmokers with wild-type EGFR and KRAS. Cancer 2009;115:1723–33.
14. Sasaki T, Rodig SJ, Chirieac LR, Janne PA. The biology and treatment of EML4-ALK non-small cell lung cancer. Eur J Cancer 2010;46:1773–80.
15. Choi YL, Takeuchi K, Soda M, Inamura K, Togashi Y, Hatano S, et al. Identification of novel isoforms of the EML4-ALK transforming gene in non-small cell lung cancer. Cancer Res 2008;68:4971–6.
16. Soda M, Takada S, Takeuchi K, Choi YL, Enomoto M, Ueno T, et al. A mouse model for EML4-ALK-positive lung cancer. Proc Natl Acad Sci U S A 2008;105:19893–7.
17. Kwak EL, Bang YJ, Camidge DR, Shaw AT, Solomon B, Maki RG, et al. Anaplastic lymphoma kinase inhibition in non-small-cell lung cancer. N Engl J Med 2011;363:1693–703.
18. Bromberg JF, Wrzeszczynska MH, Devgan G, Zhao Y, Pestell RG, Albanese C, et al. Stat3 as an oncogene. Cell 1999;98:295–303.
19. Okamoto K, Okamoto I, Okamoto W, Tanaka K, Takezawa K, Kuwata K, et al. Role of survivin in EGFR tyrosine kinase inhibitor-induced apoptosis in EGFR mutation-positive non-small cell lung cancer. Cancer Res 2010;70:10402–10.
20. Okamoto W, Okamoto I, Tanaka K, Hatashita E, Yamada Y, Kuwata K, et al. TAK-701, a humanized monoclonal antibody to HGF, reverses gefitinib resistance induced by tumor-derived HGF in non-small cell lung cancer with an EGFR mutation. Mol Cancer Ther 2010;10:2785–92.
21. Tanaka K, Arao T, Maegawa M, Matsumoto K, Kaneda H, Kudo K, et al. SRPX2 is overexpressed in gastric cancer and promotes cellular migration and adhesion. Int J Cancer 2009;124:1072–80.
22. Bai RY, Ouyang T, Miething C, Morris SW, Peschel C, Duyster J. Nucleophosmin-anaplastic lymphoma kinase associated with anaplastic large-cell lymphoma activates the phosphatidylinositol 3-kinase/Akt antiapoptotic signaling pathway. Blood 2000;96:4319–27.
23. Polgar D, Leisser C, Maier S, Strasser S, Ruger B, Dettke M, et al. Truncated ALK derived from chromosomal translocation t(2;5)(p23;q35) binds to the SH3 domain of p85-PI3K. Mutat Res 2005;570:9–15.
24. Slupianek A, Nieborowska-Skorska M, Hoser G, Morrione A, Majewski M, Xue L, et al. Role of phosphatidylinositol 3-kinase-Akt pathway in nucleophosmin/anaplastic lymphoma kinase-mediated lymphomagenesis. Cancer Res 2001;61:2194–9.
25. Rassidakis GZ, Feretzaki M, Atwell C, Grammatikakis I, Lin Q, Lai R, et al. Inhibition of Akt increases p27Kip1 levels and induces cell cycle arrest in anaplastic large cell lymphoma. Blood 2005;105:827–9.
26. Galkin AV, Melnick JS, Kim S, Hood TL, Li N, Li L, et al. Identification of NVP-TAE684, a potent, selective, and efficacious inhibitor of NPM-ALK. Proc Natl Acad Sci U S A 2007;104:270–5.
27. Crockett DK, Lin Z, Elenitoba-Johnson KS, Lim MS. Identification of NPM-ALK interacting proteins by tandem mass spectrometry. Oncogene 2004;23:2617–29.
28. Marzec M, Kasprzycka M, Liu X, Raghunath PN, Wlodarski P, Wasik MA. Oncogenic tyrosine kinase NPM/ALK induces activation of the MEK/ERK signaling pathway independently of c-Raf. Oncogene 2007;26:813–21.
29. Amin HM, McDonnell TJ, Ma Y, Lin Q, Fujio Y, Kunisada K, et al. Selective inhibition of STAT3 induces apoptosis and G(1) cell cycle arrest in ALK-positive anaplastic large cell lymphoma. Oncogene 2004;23:5426–34.
30. Zamo A, Chiarle R, Piva R, Howes J, Fan Y, Chilosi M, et al. Anaplastic lymphoma kinase (ALK) activates Stat3 and protects hematopoietic cells from cell death. Oncogene 2002;21:1038–47.
31. Shi X, Franko B, Frantz C, Amin HM, Lai R. JSI-124 (cucurbitacin I) inhibits Janus kinase-3/signal transducer and activator of transcription-3 signalling, downregulates nucleophosmin-anaplastic lymphoma kinase (ALK), and induces apoptosis in ALK-positive anaplastic large cell lymphoma cells. Br J Haematol 2006;135:26–32.
32. Han Y, Amin HM, Franko B, Frantz C, Shi X, Lai R. Loss of SHP1 enhances JAK3/STAT3 signaling and decreases proteosome degradation of JAK3 and NPM-ALK in ALK +anaplastic large-cell lymphoma. Blood 2006;108:2796–803.
33. Chiarle R, Simmons WJ, Cai H, Dhall G, Zamo A, Raz R, et al. Stat3 is required for ALK-mediated lymphomagenesis and provides a possible therapeutic target. Nat Med 2005;11:623–9.
34. McDermott U, Iafrate AJ, Gray NS, Shioda T, Classon M, Maheswaran S, et al. Genomic alterations of anaplastic lymphoma kinase may sensitize tumors to anaplastic lymphoma kinase inhibitors. Cancer Res 2008;68:3389–95.
35. Chen L, Willis SN, Wei A, Smith BJ, Fletcher JI, Hinds MG, et al. Differential targeting of prosurvival Bcl-2 proteins by their BH3-only ligands allows complementary apoptotic function. Mol Cell 2005;17:393–403.
36. Costa DB, Halmos B, Kumar A, Schumer ST, Huberman MS, Boggon TJ, et al. BIM mediates EGFR tyrosine kinase inhibitor-induced apoptosis in lung cancers with oncogenic EGFR mutations. PLoS Med 2007;4:1669–79; discussion 1680.
37. Cragg MS, Kuroda J, Puthalakath H, Huang DC, Strasser A. Gefitinib-induced killing of NSCLC cell lines expressing mutant EGFR requires BIM and can be enhanced by BH3 mimetics. PLoS Med 2007;4:1681–89; discussion 1690.
38. Gong Y, Somwar R, Politi K, Balak M, Chmielecki J, Jiang X, et al. Induction of BIM is essential for apoptosis triggered by EGFR kinase inhibitors in mutant EGFR-dependent lung adenocarcinomas. PLoS Med 2007;4:e294.
39. Hengartner MO. The biochemistry of apoptosis. Nature 2000;407:770–6.
40. Aoki Y, Feldman GM, Tosato G. Inhibition of STAT3 signaling induces apoptosis and decreases survivin expression in primary effusion lymphoma. Blood 2003;101:1535–42.

Lung Cancer xxx (2010) xxx–xxx

Contents lists available at ScienceDirect

Lung Cancer

journal homepage: www.elsevier.com/locate/lungcan

Single-agent gefitinib with concurrent radiotherapy for locally advanced non-small cell lung cancer harboring mutations of the epidermal growth factor receptor

Isamu Okamoto[a,*], Toshiaki Takahashi[b], Hiroaki Okamoto[c], Kazuhiko Nakagawa[a], Koshiro Watanabe[c], Kiyoshi Nakamatsu[d], Yasumasa Nishimura[d], Masahiro Fukuoka[e], Nobuyuki Yamamoto[b]

[a] Department of Medical Oncology, Kinki University School of Medicine, Osaka, Japan
[b] Division of Thoracic Oncology, Shizuoka Cancer Center Hospital, Shizuoka, Japan
[c] Department of Respiratory Medicine and Medical Oncology, Yokohama Municipal Citizen's Hospital, Yokohama, Japan
[d] Department of Radiation Oncology, Kinki University School of Medicine, Osaka, Japan
[e] Cancer Center, Izumi Municipal Hospital, Osaka, Japan

ARTICLE INFO

Article history:
Received 10 June 2010
Received in revised form 11 August 2010
Accepted 16 August 2010

Key words:
Non-small cell lung cancer
Locally advanced
Gefitinib
Radiotherapy
EGFR mutation

ABSTRACT

Introduction: A feasibility study was performed to examine the safety and toxicity profile of daily gefitinib (250 mg) administration with concurrent definitive thoracic radiation therapy (TRT) in patients with unresectable non-small cell lung cancer (NSCLC) of stage III.
Methods: Patients received a 14-day induction therapy with gefitinib at 250 mg daily. TRT was initiated on day 15 in 2-Gy fractions administered five times weekly to a total dose of 60 Gy. The primary end point of the study was the rate of treatment completion. Mutation status of the epidermal growth factor receptor gene (*EGFR*) was evaluated for patients with available tumor specimens.
Results: Nine eligible patients enrolled in the study received induction gefitinib monotherapy. Two patients were unable to begin TRT because of the development of progressive disease during the first 2 weeks of the protocol. Three of the remaining seven patients treated with gefitinib and concurrent TRT were unable to complete the planned treatment (two because of pulmonary toxicity and one because of progressive disease), and the study was therefore closed according to the protocol definition. Tumor samples were available for eight patients. *EGFR* mutations (deletion in exon 19) were detected in two patients, both of whom achieved a partial response and exhibited an overall survival of >5 years.
Conclusions: Our results do not support further trials of gefitinib and TRT for unselected NSCLC patients. This therapeutic strategy may hold promise, however, for locally advanced NSCLC in patients with sensitizing *EGFR* mutations.

1. Introduction

Lung cancer remains the most common cause of cancer-related mortality worldwide [1]. Non-small cell lung cancer (NSCLC) is a heterogeneous disease that accounts for ~80% of lung cancer cases, and about one-third of individuals with newly diagnosed NSCLC present with locally advanced disease not amenable to curative resection [2]. The current standard of care for patients with unresectable locally advanced NSCLC is concurrent chemotherapy and definitive thoracic radiation therapy (TRT); however, most treated individuals experience disease recurrence, with the 5-year survival rate being only ~20% [3–5]. Further improvement in treatment outcome for patients with locally advanced NSCLC will require the development of more effective combined-modality therapies.

The expression and activity of the epidermal growth factor receptor (EGFR) are important determinants of radiation sensitivity in several cancers including NSCLC [6–9]. Irradiation of tumor cells has been shown to activate EGFR via ligand-dependent and ligand-independent mechanisms, possibly accounting for the radiation-induced acceleration of tumor cell repopulation and the development of radioresistance [9,10]. Such radiation-induced activation of EGFR-dependent processes provides a rationale for combined treatment with radiation and EGFR inhibitors. Indeed, preclinical models have shown that EGFR inhibition enhances the antitumor activity of radiation [11–14]. Gefitinib is a small-molecule tyrosine kinase inhibitor (TKI) of EGFR that competes with ATP for binding to the tyrosine kinase pocket of the receptor, thereby inhibiting receptor tyrosine kinase activity and EGFR

* Corresponding author at: Department of Medical Oncology, Kinki University School of Medicine, 377-2 Ohno-higashi, Osaka-Sayama, Osaka 589-8511, Japan. Tel.: +81 72 366 0221; fax: +81 72 360 5000.
E-mail address: chi-okamoto@dotd.med.kindai.ac.jp (I. Okamoto).

0169-5002/$ – see front matter © 2010 Elsevier Ireland Ltd. All rights reserved.
doi:10.1016/j.lungcan.2010.08.016

signaling pathways [15]. Although several clinical studies have examined the use of gefitinib in patients with advanced or metastatic NSCLC [15–17], no data have been available regarding the efficacy of single-agent gefitinib combined with TRT in individuals with locally advanced NSCLC. We have now performed a feasibility study of gefitinib with concurrent TRT in patients with locally advanced NSCLC in order to establish the safety and toxicity profile of this therapeutic strategy. Midway through this study, the discovery of somatic mutations in *EGFR* and of the association of such mutations with a high response rate to EGFR-TKIs had a profound impact on the treatment of metastatic NSCLC [18–20]. We therefore examined the potential relation between the presence of *EGFR* mutations as detected in diagnostic biopsy specimens and treatment outcome.

2. Materials and methods

2.1. Eligibility criteria

Patients with pathologically confirmed unresectable NSCLC of stage III were eligible for enrollment in the study, whereas those with T3N1 disease, contralateral mediastinal lymph node metastasis, malignant pleural effusion, pericardial effusion, or pleural dissemination were excluded. Additional eligibility criteria included no previous disease treatment, the presence of any measurable lesion, an Eastern Cooperative Oncology Group performance status score of 0–1, an age of ≤75 years, no history of malignancy within the previous 5 years, a leukocyte count of ≥4000/μL, a platelet count of ≥100,000/μL, a hemoglobin level of ≥9 g/dL, serum aspartate aminotransferase (AST) and alanine aminotransferase (ALT) levels of ≤50 IU/L, a serum creatinine concentration of ≤1.2 mg/dL, and an arterial oxygen pressure (PaO_2) of ≥70 mm Hg. Patients were excluded if they had interstitial pneumonitis, uncontrolled diabetes mellitus, or any serious underlying disease or complications. Staging workup included a chest radiograph, computed tomography (CT) scans of the chest and abdomen, either a CT scan or magnetic resonance imaging of the brain, and a radioisotopic bone scan. All subjects provided written informed consent to participation in the study, which was approved by the Institutional Review Board of each participating center (Kinki University School of Medicine and Yokohama Municipal Citizen's Hospital) and was performed in accordance with the Declaration of Helsinki.

2.2. Gefitinib therapy

Patients started taking 250 mg of gefitinib per day orally 14 days before initiation of TRT and continued doing so during TRT. At the completion of TRT, patients were maintained on gefitinib at 250 mg daily until evidence of disease progression or toxicity for up to 1 year. In the event of development of toxicities of grade 2 or higher, gefitinib was postponed until the toxicities had improved to grade 1 or lower. In the case that cessation of TRT was warranted, gefitinib was withheld until resumption of the remainder of the concurrent phase of the treatment. If patients experienced toxicities of grade 3 or higher or any grade of pneumonitis related to gefitinib, the treatment was terminated.

2.3. Radiation therapy

TRT was administered from day 15 of gefitinib using a linear accelerator photon beam of 6-MV or more. Three-dimensional (3D) treatment planning systems using computed tomography were used at both hospitals. Lung inhomogeneity correction was not performed in dose calculation. Radiation doses were specified at the center of the target volume.

The primary tumor and involved nodal disease received 60 Gy in 2-Gy fractions over 6 weeks. The initial 40 Gy was delivered to clinical target volume 1 (CTV1), and the final 20 Gy was delivered to a reduced volume defined as clinical target volume 2 (CTV2). CTV1 included the primary tumor, ipsilateral hilum, and mediastinal nodal areas from the paratracheal (#2) to subcarinal lymph nodes (#7). The contralateral hilum was not included in CTV1. The supraclavicular areas were not to be treated routinely, but could be treated when supraclavicular nodes were involved. For the primary tumors and the involved lymph nodes of 1 cm in the shortest diameter, a margin of 1.5–2 cm was added. CTV2 included only the primary tumor and the involved lymph nodes with a margin of 0.5–1 cm. The spinal cord was excluded from the fields for CTV2 by appropriate methods such as the oblique opposing method. Appropriate PTV margin and leaf margin were added for CTV1 and CTV2.

The objectives were to restrict the relative volume of the normal lung treated with a dose of >20 Gy (V20) to <35%, and the maximum spinal cord dose was restricted to <44 Gy. If patients experienced grade 3/4 esophagitis or dermatitis, pyrexia of 38 °C or more, or a decrease in PaO2 of >10 mm Hg compared to baseline, TRT was withheld until esophagitis or dermatitis improved to grade 2 or clinically acceptable toxicity level. If patients experienced grade 1 or more pneumonitis related to gefitinib, TRT was terminated. Assessment of toxicity and response All eligible patients who received any portion of the treatment regimen were considered assessable for toxicity and response. A CT scan of the chest was performed within 14 days of initiation of study treatment and was repeated on day 14 of gefitinib monotherapy in order to exclude individuals with disease progression or pneumonitis related to gefitinib. Chest X-rays, complete blood counts, and blood chemistry analysis were performed weekly until completion of TRT. Toxicities were assessed with the use of the National Cancer Institute Common Terminology Criteria for Adverse Events v2.0. Treatment response was evaluated according to the Response Evaluation Criteria in Solid Tumors [21]. The initial tumor response was defined as the best response recorded within 3 months after the start of treatment. Progression-free survival (PFS) and overall survival (OS) were calculated from the date of registration in the study until the first documented instance of disease progression or death, respectively, with the use of the Kaplan–Meier method. Follow-up assessments included a posttreatment CT scan at 4–12 weeks after completion of TRT.

2.5. Study design and statistical considerations

The primary end point of the study was the rate of treatment completion. Complete treatment delivery was defined as completion of the planned 60 Gy of TRT within 63 days and administration of gefitinib for >3 weeks during TRT. We selected a 90% completion rate as a desirable target level and a 75% completion rate as uninteresting with an alpha error of 0.1 and a power of 0.8, resulting in a requirement for 28 patients. If 24 or more treatment completions were achieved among the 28 total assessable patients, the treatment was considered worthy of further consideration. Secondary end points included estimation of the objective response rate as well as of PFS and OS.

2.6. Analysis of EGFR mutation

Tumor specimens (embedded in paraffin) were collected during previous diagnostic procedures. *EGFR* mutations that confer sensitivity to EGFR-TKIs were identified by the PCR-Invader method (BML, Tokyo, Japan). Some patients had already died before the initiation of our genetic analysis, preventing us from obtaining informed consent. The Institutional Review Boards therefore approved our study protocol with the conditions that samples

Please cite this article in press as: Okamoto I, et al. Single-agent gefitinib with concurrent radiotherapy for locally advanced non-small cell lung cancer harboring mutations of the epidermal growth factor receptor. Lung Cancer (2010), doi:10.1016/j.lungcan.2010.08.016

Table 1
Treatment details and outcomes for the study cohort.

Patient	Age/sex	Smoking history	Histology	TNM stage	Gefitinib (total days of therapy)	TRT (total dose, Gy)	Treatment completion	Initial tumor response	Pattern of recurrence	PFS (months)	OS (months)	*EGFR* status
1	68/M	48/day × 20 years	Large cell	T1N2	13	0	No	PD	Locoregional	0.5	6.3	Wild type
2	71/M	60/day × 60 years	NSCLC	T2N3	58	34	No	SD	Locoregional + distant (bone)	5.7	5.9	Wild type
3	69/M	50/day × 60 years	Adeno	T1N2	134	60	Yes	PR	Distant (bone)	4.5	5.9	Wild type
4	56/M	41/day × 40 years	Adeno	T4N0	604	60	Yes	PR	None	73.6+	NA	NA
5	62/M	30/day × 30 years	Adeno	T1N2	107	60	Yes	PR	Distant (brain)	19.6	67.5	Exon 19 del
6	59/M	40/day × 40 years	Adeno	T1N2	13	0	No	PD	Locoregional	0.5	3.1	Wild type
7	62/F	None	Adeno	T4N1	302	60	Yes	PR	Distant (brain)	14.6	63.7+	Exon 19 del
8	63/M	20/day × 20 years	Adeno	T4N2	23	60	No	PD	Locoregional	2.4	11.5	Wild type
9	67/M	40/day × 15 years	Squamous	T4N2	50	46	No	PD	Locoregional	1.9	2.5	Wild type

NA, not applicable.

Table 2
Toxicity of induction gefitinib monotherapy ($n = 9$).

Toxicity	Grade			
	1	2	3	4
Hematologic				
Leukopenia	1	0	0	0
Neutropenia	0	0	0	0
Anemia	4	0	0	0
Thrombocytopenia	1	0	0	0
Febrile neutropenia	NA	NA	0	0
Nonhematologic				
Fever	1	0	0	0
Fatigue	0	1	0	0
Dry skin	1	0	0	0
Skin rash	5	0	0	0
Elevated AST	2	0	0	0

NA, not applicable.

would be processed anonymously and analyzed only for somatic mutations (not germline mutations) and that the study would be publicly disclosed, according to the Ethical Guidelines for Human Genome Research published by the Ministry of Education, Culture, Sports, Science, and Technology, the Ministry of Health, Labor, and Welfare, and the Ministry of Economy, Trade, and Industry of Japan.

3. Results

3.1. Patient characteristics

Between August 2003 and January 2005, nine eligible patients were enrolled in the study at the two participating centers (Table 1). The patients included one women and eight men, with a median age of 63 years (range, 56–71). Five patients had stage IIIA disease and four had stage IIIB disease. Histological subtypes included adenocarcinoma in six patients, squamous cell carcinoma in one patient, large cell carcinoma in one patient, and unspecified NSCLC in one patient. Eight of the nine patients were current smokers.

3.2. Toxicity

Safety analysis included all nine patients who received at least one dose of gefitinib. All adverse events were monitored continuously during treatment and for 2 years after the end of treatment. Five patients did not complete the planned trial therapy and subsequent enrollment was stopped according to the protocol definition (Table 1). Two subjects (patients 1 and 6) showed progression of their primary lung tumors on planned CT evaluation on day 14 of gefitinib monotherapy and were thus unable to start TRT according to the protocol. Patient 2 manifested acutely deteriorating dyspnea and hypoxemia with a PaO_2 of 46.0 mm Hg after 24 days of gefitinib therapy and 34 Gy of radiotherapy. A CT scan of the chest revealed diffuse ground-glass opacities that were consistent with the known pulmonary toxicity of gefitinib. Discontinuation of gefitinib and radiotherapy and initiation of steroid treatment resulted in improvement of the patient's condition. Patient 8 presented with pneumonitis of grade 1 at 23 days after initiation of gefitinib. This condition was interpreted as a gefitinib-related toxicity, and the patient had gefitinib withdrawn but continued with radiotherapy up to 60 Gy without further toxicity. V20 parameters in the two patients (patients 2 and 8) who suffered from pulmonary toxicities were 25 and 20%, respectively. Patient 9 discontinued the trial treatment after 46 Gy of radiotherapy because of enlargement of the primary lung lesion at 50 days after initiation of gefitinib administration.

Please cite this article in press as: Okamoto I, et al. Single-agent gefitinib with concurrent radiotherapy for locally advanced non-small cell lung cancer harboring mutations of the epidermal growth factor receptor. Lung Cancer (2010), doi:10.1016/j.lungcan.2010.08.016

Table 3
Acute toxicity during concurrent gefitinib and TRT (n = 7).

Toxicity	Grade			
	1	2	3	4
Hematologic				
Leukopenia	3	1	0	0
Neutropenia	1	0	0	0
Anemia	1	1	0	0
Thrombocytopenia	2	0	0	0
Febrile neutropenia	NA	NA	0	0
Nonhematologic				
Esophagitis	5	1	0	0
Skin rash	4	1	0	0
Elevated ALT	0	2	3	0
Elevated AST	1	1	3	0
Fatigue	3	1	0	0
Anorexia	1	1	0	0
Fever	1	1	0	0
Dry skin	2	0	0	0
Pneumonitis	1	0	1	0

NA, not applicable.

The incidence of adverse events of all grades during the entire treatment period is shown in Tables 2 and 3. Although esophagitis and skin rash were most commonly encountered, these conditions were only of grade 1 or 2. Toxicities of grade 3 occurred in four patients: an increase in the serum levels of hepatic transaminases in three patients and pneumonitis in one patient. No hematologic toxicities of grade 3 or 4 were observed. There were no treatment-related deaths.

3.3. Treatment outcomes

At the time of analysis, two patients were still alive and seven patients had died. Eight patients had progressed, four experiencing local progression, three distant progression, and one local and distant progression (Table 1). All four patients who completed the planned treatment schedule experienced a partial response at the end of combined treatment, with a PFS of 4.5, 14.6, 19.6, and ≥73.6 months. Three of these four patients were alive >60 months without local recurrence from entry into the study.

3.4. EGFR mutation analysis

Tumor specimens were available for eight of the nine patients enrolled in the study and were successfully tested for *EGFR* mutations. Sensitizing *EGFR* mutations were detected in two individuals (patients 5 and 7), both of whom completed the planned trial treatment and exhibited an OS of >5 years.

4. Discussion

In this study, we sought to investigate the tolerability and safety of gefitinib when combined with definitive TRT in patients with locally advanced NSCLC. Given that five of the first nine patients enrolled in the study were unable to complete the planned treatment (two developing pulmonary toxicity and three progressive disease), the combination of gefitinib with TRT was not considered feasible in unselected patients according to the protocol definition and the study was closed.

Life-threatening interstitial lung disease (ILD) related to gefitinib has previously been identified as the most problematic toxicity of this drug, with an incidence thought to be ~4% and with about one-third of the cases being fatal in Japan [22,23]. The predictive risk factors for ILD development include male sex, smoking, and the existence of idiopathic pulmonary fibrosis [22]. In the present study, two male smokers experienced pneumonitis (one of the grade 3 and one of the grade 1) during concurrent gefitinib administration and TRT, both cases necessitating discontinuation of gefitinib treatment. It remains unclear whether TRT increases the risk for development of gefitinib-related ILD. We have recently completed a multicenter single-arm trial [Japan Clinical Oncology Group (JCOG) 0402] consisting of induction cisplatin and vinorelbine followed by gefitinib and concurrent TRT in patients with locally advanced NSCLC [5]. Eligibility for enrollment in the JCOG trial, the criteria for which were changed midway through the study to reduce the risk of gefitinib-induced ILD, was limited to individuals with adenocarcinoma who were either never-smokers or former light-smokers. Safety data for concurrent gefitinib and TRT in such selected patients are eagerly awaited. With the exception of pulmonary adverse events possibly resulting from gefitinib treatment, the combination of gefitinib and TRT did not show any unexpected toxicity, with no marked increase in radiation-induced toxicities, in the present study. Other recent studies that incorporated EGFR-TKIs into chemoradiation for locally advanced NSCLC also showed that such combination therapy was safe and feasible [24–26].

In the present study, gefitinib monotherapy was instigated 2 weeks before the onset of concurrent TRT because of concern about the relatively high risk for development of gefitinib-induced ILD during the initial exposure to the drug [22,23]. The study protocol also required assessment of antitumor effect after the induction gefitinib monotherapy, and, indeed, two patients were withdrawn before the start of concurrent TRT because of the development of progressive disease. This approach was adopted to avoid ineffective therapy given that platinum-based chemotherapy with concurrent TRT has been established as the standard treatment for locally advanced NSCLC [3]. At the time the trial was initiated, clinical data showing the association between sensitizing *EGFR* mutations and response to EGFR-TKIs were unavailable. Several prospective clinical trials of EGFR-TKI treatment for NSCLC patients with *EGFR* mutations have subsequently revealed radiographic response rates of 55–91% [27–36]. Furthermore, *EGFR* mutations are more frequent in females, individuals with no history of smoking, and patients with adenocarcinoma, all of which characteristics are associated with a low risk of gefitinib-induced ILD [22,37,38]. These findings suggest that patient selection on the basis of *EGFR* mutation status can minimize the risk of gefitinib-related ILD and maximize the efficacy of gefitinib combined with TRT.

Unique to our present study is the post hoc analysis of *EGFR* mutation. We detected *EGFR* mutations in two of the eight patients with available tumor specimens, and both of these individuals survived for >5 years. These two *EGFR* mutation-positive patients (patients 5 and 7) presented with brain metastasis as the first site of treatment failure, consistent with previous reports that the brain is a frequent site of recurrence after curative multimodality approaches for locally advanced NSCLC [39]. Patient 5 were treated with gamma knife radiosurgery for his solitary brain metastasis at 19.6 months after the start of protocol treatment; however he died of meningeal carcinomatosis with an overall survival of 67.5 months. Patient 7 received gamma knife radiosurgery for brain metastases and thereafter remained well without recurrence. It is noted that both of these *EGFR* mutation-positive patients have never experienced local progression. These clinical courses differ from those of metastatic *EGFR* mutation-positive NSCLC, for which most tumors are initially responsive to EGFR-TKIs but almost invariably develop resistance to the drug, leading to recurrence and death. Preclinical studies have shown that NSCLC cells harboring *EGFR* mutations have a predominantly radiosensitive phenotype associated with a delay in the repair of radiation-induced DNA damage, defective radiation-induced arrest of DNA synthesis or mitosis, and a pronounced increase

Please cite this article in press as: Okamoto I, et al. Single-agent gefitinib with concurrent radiotherapy for locally advanced non-small cell lung cancer harboring mutations of the epidermal growth factor receptor. Lung Cancer (2010), doi:10.1016/j.lungcan.2010.08.016

in the frequency of radiation-induced apoptosis [40]. Given these radiosensitivity characteristics, *EGFR* mutation-positive NSCLC patients treated with radiotherapy may avoid the emergence of resistance to gefitinib. The implications of these findings for optimal design of future trials of molecularly based combined-modality treatments including EGFR-TKIs and radiotherapy are under consideration.

In conclusion, the combination of gefitinib with TRT for locally advanced NSCLC is not recommended for unselected patients because of concerns with efficacy and toxicity. We did, however, observe that *EGFR* mutation-positive patients had a favorable clinical outcome with this combination therapy. We have recently completed phase III trials in *EGFR* mutation-positive patients with advanced NSCLC and found that first-line gefitinib monotherapy was associated with a significantly better response rate and PFS compared with platinum-based chemotherapy [41]. Although the number of patients in the current study was too small to be able to draw firm conclusions, our preliminary findings suggest that TRT combined with gefitinib in place of platinum-based chemotherapy is a potential option for the treatment of patients with locally advanced NSCLC who have sensitizing *EGFR* mutations. Further development of EGFR-TKI treatment in combination with TRT in molecularly selected patients is warranted.

Conflict of interest

The authors declare no actual or potential conflicts of interest.

Acknowledgment

This work was supported in part by a Grand-in-Aid for Cancer Research from the Ministry of Health, Labor and Welfare of Japan.

References

[1] Jemal A, Siegel R, Ward E, Hao Y, Xu J, Thun MJ. Cancer statistics, 2009. CA Cancer J Clin 2009;59:225–49.
[2] Blackstock AW, Govindan R. Definitive chemoradiation for the treatment of locally advanced non small-cell lung cancer. J Clin Oncol 2007;25: 4146–52.
[3] Pfister DG, Johnson DH, Azzoli CG, Sause W, Smith TJ, Baker Jr S, et al. American Society of Clinical Oncology treatment of unresectable non-small-cell lung cancer guideline: update 2003. J Clin Oncol 2004;22:330–53.
[4] Furuse K, Fukuoka M, Kawahara M, Nishikawa H, Takada Y, Kudoh S, et al. Phase III study of concurrent versus sequential thoracic radiotherapy in combination with mitomycin, vindesine, and cisplatin in unresectable stage III non-small-cell lung cancer. J Clin Oncol 1999;17:2692–9.
[5] Okamoto I. Overview of chemoradiation clinical trials for locally advanced non-small cell lung cancer in Japan. Int J Clin Oncol 2008;13:112–6.
[6] Liang K, Ang KK, Milas L, Hunter N, Fan Z. The epidermal growth factor receptor mediates radioresistance. Int J Radiat Oncol Biol Phys 2003;57:246–54.
[7] Milas L, Mason KA, Ang KK. Epidermal growth factor receptor and its inhibition in radiotherapy: in vivo findings. Int J Radiat Biol 2003;79:539–45.
[8] Harari PM, Huang SM. Epidermal growth factor receptor modulation of radiation response: preclinical and clinical development. Semin Radiat Oncol 2002;12:21–6.
[9] Schmidt-Ullrich RK, Mikkelsen RB, Dent P, Todd DG, Valerie K, Kavanagh BD, et al. Radiation-induced proliferation of the human A431 squamous carcinoma cells is dependent on EGFR tyrosine phosphorylation. Oncogene 1997;15:1191–7.
[10] Lammering G, Hewit TH, Hawkins WT, Contessa JN, Reardon DB, Lin PS, et al. Epidermal growth factor receptor as a genetic therapy target for carcinoma cell radiosensitization. J Natl Cancer Inst 2001;93:921–9.
[11] Chinnaiyan P, Huang S, Vallabhaneni G, Armstrong E, Varambally S, Tomlins SA, et al. Mechanisms of enhanced radiation response following epidermal growth factor receptor signaling inhibition by erlotinib (Tarceva). Cancer Res 2005;65:3328–35.
[12] Raben D, Helfrich B, Chan DC, Ciardiello F, Zhao L, Franklin W, et al. The effects of cetuximab alone and in combination with radiation and/or chemotherapy in lung cancer. Clin Cancer Res 2005;11:795–805.
[13] She Y, Lee F, Chen J, Haimovitz-Friedman A, Miller VA, Rusch VR, et al. The epidermal growth factor receptor tyrosine kinase inhibitor ZD1839 selectively potentiates radiation response of human tumors in nude mice, with a marked improvement in therapeutic index. Clin Cancer Res 2003;9:3773–8.
[14] Bonner JA, Raisch KP, Trummell HQ, Robert F, Meredith RF, Spencer SA, et al. Enhanced apoptosis with combination C225/radiation treatment serves as the impetus for clinical investigation in head and neck cancers. J Clin Oncol 2000;18:47S–53S.
[15] Okamoto I. Epidermal growth factor receptor in relation to tumor development: EGFR-targeted anticancer therapy. FEBS J 2010;277:309–315.
[16] Jiang H. Overview of gefitinib in non-small cell lung cancer: an Asian perspective. Jpn J Clin Oncol 2009;39:137–50.
[17] Saijo N, Takeuchi M, Kunitoh H. Reasons for response differences seen in the V15-32, INTEREST and IPASS trials. Nat Rev Clin Oncol 2009;6:287–94.
[18] Lynch TJ, Bell DW, Sordella R, Gurubhagavatula S, Okimoto RA, Brannigan BW, et al. Activating mutations in the epidermal growth factor receptor underlying responsiveness of non-small-cell lung cancer to gefitinib. N Engl J Med 2004;350:2129–39.
[19] Paez JG, Janne PA, Lee JC, Tracy S, Greulich H, Gabriel S, et al. EGFR mutations in lung cancer: correlation with clinical response to gefitinib therapy. Science 2004;304:1497–500.
[20] Pao W, Miller V, Zakowski M, Doherty J, Politi K, Sarkaria I, et al. EGF receptor gene mutations are common in lung cancers from "never smokers" and are associated with sensitivity of tumors to gefitinib and erlotinib. Proc Natl Acad Sci USA 2004;101:13306–11.
[21] Therasse P, Arbuck SG, Eisenhauer EA, Wanders J, Kaplan RS, Rubinstein L, et al. New guidelines to evaluate the response to treatment in solid tumors, European Organization for Research and Treatment of Cancer, National Cancer Institute of the United States, National Cancer Institute of Canada. J Natl Cancer Inst 2000;92:205–16.
[22] Ando M, Okamoto I, Yamamoto N, Takeda K, Tamura K, Seto T, et al. Predictive factors for interstitial lung disease, antitumor response, and survival in non-small-cell lung cancer patients treated with gefitinib. J Clin Oncol 2006;24:2549–56.
[23] Kudoh S, Kato H, Nishiwaki Y, Fukuoka M, Nakata K, Ichinose Y, et al. Interstitial lung disease in Japanese patients with lung cancer: a cohort and nested case–control study. Am J Respir Crit Care Med 2008;177:1348–57.
[24] Stinchcombe TE, Morris DE, Lee CB, Moore DT, Hayes DN, Halle JS, et al. Induction chemotherapy with carboplatin, irinotecan, and paclitaxel followed by high dose three-dimension conformal thoracic radiotherapy (74 Gy) with concurrent carboplatin, paclitaxel, and gefitinib in unresectable stage IIIA and stage IIIB non-small cell lung cancer. J Thorac Oncol 2008;3:250–7.
[25] Choong NW, Mauer AM, Haraf DJ, Lester E, Hoffman PC, Kozloff M, et al. Phase I trial of erlotinib-based multimodality therapy for inoperable stage III non-small cell lung cancer. J Thorac Oncol 2008;3:1003–11.
[26] Center B, Petty WJ, Ayala D, Hinson WH, Lovato J, Capellari J, et al. A phase I study of gefitinib with concurrent dose-escalated weekly docetaxel and conformal three-dimensional thoracic radiation followed by consolidative docetaxel and maintenance gefitinib for patients with stage III non-small cell lung cancer. J Thorac Oncol 2010;5:69–74.
[27] Inoue A, Suzuki T, Fukuhara T, Maemondo M, Kimura Y, Morikawa N, et al. Prospective phase II study of gefitinib for chemotherapy-naive patients with advanced non-small-cell lung cancer with epidermal growth factor receptor gene mutations. J Clin Oncol 2006;24:3340–6.
[28] Asahina H, Yamazaki K, Kinoshita I, Sukoh N, Harada M, Yokouchi H, et al. A phase II trial of gefitinib as first-line therapy for advanced non-small cell lung cancer with epidermal growth factor receptor mutations. Br J Cancer 2006;95:998–1004.
[29] Sutani A, Nagai Y, Udagawa K, Uchida Y, Koyama N, Murayama Y, et al. Gefitinib for non-small-cell lung cancer patients with epidermal growth factor receptor gene mutations screened by peptide nucleic acid-locked nucleic acid PCR clamp. Br J Cancer 2006;95:1483–9.
[30] Yoshida K, Yatabe Y, Park JY, Shimizu J, Horio Y, Matsuo K, et al. Prospective validation for prediction of gefitinib sensitivity by epidermal growth factor receptor gene mutation in patients with non-small cell lung cancer. J Thorac Oncol 2007;2:22–8.
[31] Sunaga N, Tomizawa Y, Yanagitani N, Iijima H, Kaira K, Shimizu K, et al. Phase II prospective study of the efficacy of gefitinib for the treatment of stage III/IV non-small cell lung cancer with EGFR mutations, irrespective of previous chemotherapy. Lung Cancer 2007;56:383–9.
[32] Tamura K, Okamoto I, Kashii T, Negoro S, Hirashima T, Kudoh S, et al. Multicentre prospective phase II trial of gefitinib for advanced non-small cell lung cancer with epidermal growth factor receptor mutations: results of the West Japan Thoracic Oncology Group trial (WJTOG0403). Br J Cancer 2008;98: 907–14.
[33] Sequist LV, Martins RG, Spigel D, Grunberg SM, Spira A, Janne PA, et al. First-line gefitinib in patients with advanced non-small-cell lung cancer harboring somatic EGFR mutations. J Clin Oncol 2008;26:2442–9.
[34] Sugio K, Uramoto H, Onitsuka T, Mizukami M, Ichiki Y, Sugaya M, et al. Prospective phase II study of gefitinib in non-small cell lung cancer with epidermal growth factor receptor gene mutations. Lung Cancer 2009;64:314–8.
[35] Morita S, Okamoto I, Kobayashi K, Yamazaki K, Asahina H, Inoue A, et al. Combined survival analysis of prospective clinical trials of gefitinib for non-small cell lung cancer with EGFR mutations. Clin Cancer Res 2009;15:4493–8.
[36] Jackman DM, Miller VA, Cioffredi LA, Yeap BY, Janne PA, Riely GJ, et al. Impact of epidermal growth factor receptor and KRAS mutations on clinical outcomes in previously untreated non-small cell lung cancer patients: results of an online tumor registry of clinical trials. Clin Cancer Res 2009;15:5267–73.
[37] Mitsudomi T, Yatabe Y. Mutations of the epidermal growth factor receptor gene and related genes as determinants of epidermal growth factor recep-

Please cite this article in press as: Okamoto I, et al. Single-agent gefitinib with concurrent radiotherapy for locally advanced non-small cell lung cancer harboring mutations of the epidermal growth factor receptor. Lung Cancer (2010), doi:10.1016/j.lungcan.2010.08.016

tor tyrosine kinase inhibitors sensitivity in lung cancer. Cancer Sci 2007;98: 1817–24.
[38] Mok TS, Wu YL, Thongprasert S, Yang CH, Chu DT, Saijo N, et al. Gefitinib or carboplatin-paclitaxel in pulmonary adenocarcinoma. N Engl J Med 2009;361:947–57.
[39] Topkan E, Yildirim BA, Selek U, Yavuz MN. Cranial prophylactic irradiation in locally advanced non-small cell lung carcinoma: current status and future perspectives. Oncology 2009;76:220–8.
[40] Das AK, Sato M, Story MD, Peyton M, Graves R, Redpath S, et al. Non-small-cell lung cancers with kinase domain mutations in the epidermal growth factor receptor are sensitive to ionizing radiation. Cancer Res 2006;66: 9601–8.
[41] Mitsudomi T, Morita S, Yatabe Y, Negoro S, Okamoto I, Tsurutani J, et al. Gefitinib versus cisplatin plus docetaxel in patients with non-small-cell lung cancer harbouring mutations of the epidermal growth factor receptor (WJTOG3405): an open label, randomised phase 3 trial. Lancet Oncol 2010;11:121–128.

Please cite this article in press as: Okamoto I, et al. Single-agent gefitinib with concurrent radiotherapy for locally advanced non-small cell lung cancer harboring mutations of the epidermal growth factor receptor. Lung Cancer (2010), doi:10.1016/j.lungcan.2010.08.016

J Gastroenterol
DOI 10.1007/s00535-010-0294-5

ORIGINAL ARTICLE—LIVER, PANCREAS, AND BILIARY TRACT

The cancer stem cell marker CD133 is a predictor of the effectiveness of S1+ pegylated interferon α-2b therapy against advanced hepatocellular carcinoma

Satoru Hagiwara · Masatoshi Kudo · Kazuomi Ueshima · Hobyung Chung · Mami Yamaguchi · Masahiro Takita · Seiji Haji · Masatomo Kimura · Tokuzo Arao · Kazuto Nishio · Ah-Mee Park · Hiroshi Munakata

Received: 23 December 2009 / Accepted: 8 July 2010

Abstract
Background Combination therapy with the oral fluoropyrimidine anticancer drug S1 and interferon is reportedly effective for the treatment of advanced hepatocellular carcinoma (HCC), but selection criteria for this therapy have not been clarified. In this study, we attempted to identify factors predicting the effectiveness of this combination therapy.
Methods Pathological specimens of HCC were collected before treatment from 31 patients with advanced HCC who underwent S1+ pegylated-interferon (PEG-IFN) α-2b therapy between January 2007 and January 2009. In these pathological specimens, the expression levels of CD133, thymidylate synthase (TS), dihydropyrimidine dehydrogenase (DPD), and interferon-receptor 2 (IFNR2) proteins were determined by Western blot assay. The presence or absence of p53 gene mutations was determined by direct sequencing. The relationships between these protein expression levels and the response rate (RR), progression-free survival (PFS), and overall survival (OS) were evaluated.
Results The CD133 protein expression level was significantly lower in the responder group than in the nonresponder group. Comparing the PFS and OS between high- and low-level CD133 expression groups ($n = 13$ and 18, respectively) revealed that both parameters were significantly prolonged in the latter group. The expression levels of TS, DPD, and IFNR2 protein and the presence of p53 gene mutations did not correlate with the RR.
Conclusions CD133 was identified as a predictor of the therapeutic effect of S1+ PEG-IFN α-2b therapy against advanced HCC.

Keywords 5-Fluorouracil · Pegylated interferon · CD133 · Cancer stem cell · Hepatocellular carcinoma

Abbreviations

5FU	5-Fluorouracil
DPD	Dihydropyrimidine dehydrogenase
HCC	Hepatocellular carcinoma
IFNR2	Interferon-receptor 2
NR	Nonresponder
OS	Overall survival
PD	Progressive disease
PEG-IFN	Pegylated interferon
PFS	Progression-free survival
PR	Partial response
RR	Response rate

S. Hagiwara · M. Kudo (✉) · K. Ueshima · H. Chung · M. Yamaguchi · M. Takita
Division of Gastroenterology and Hepatology, Department of Internal Medicine, Kinki University School of Medicine, 377-2 Ohno-Higashi, Ōsakasayama, Osaka 589-8511, Japan
e-mail: m-kudo@med.kindai.ac.jp

S. Haji
Department of Surgery, Kinki University School of Medicine, Ōsakasayama, Japan

M. Kimura
Department of Pathology, Kinki University School of Medicine, Ōsakasayama, Japan

T. Arao · K. Nishio
Department of Genome Biology, Kinki University School of Medicine, Ōsakasayama, Japan

A.-M. Park · H. Munakata
Department of Biochemistry, Kinki University School of Medicine, Ōsakasayama, Japan

Published online: 04 August 2010